BioSim
EU NETWORK OF EXCELLENCE

Mathematical Modeling of Complex Biomedical Systems

Erik Mosekilde
Department of Physics
The Technical University of Denmark
Patras 1, July 2011

DTU

Complex Biomedical Systems

1. *Modeling and Simulation in Biomedical Research and Health Care*
2. Role of Nonlinear Dynamic Phenomena in Living Systems
3. Synchronization and Chaos in Nephron Autoregulation
4. Bifurcation Structures in Interacting Biological Units
5. Exercises

New, Safe Medicines Faster

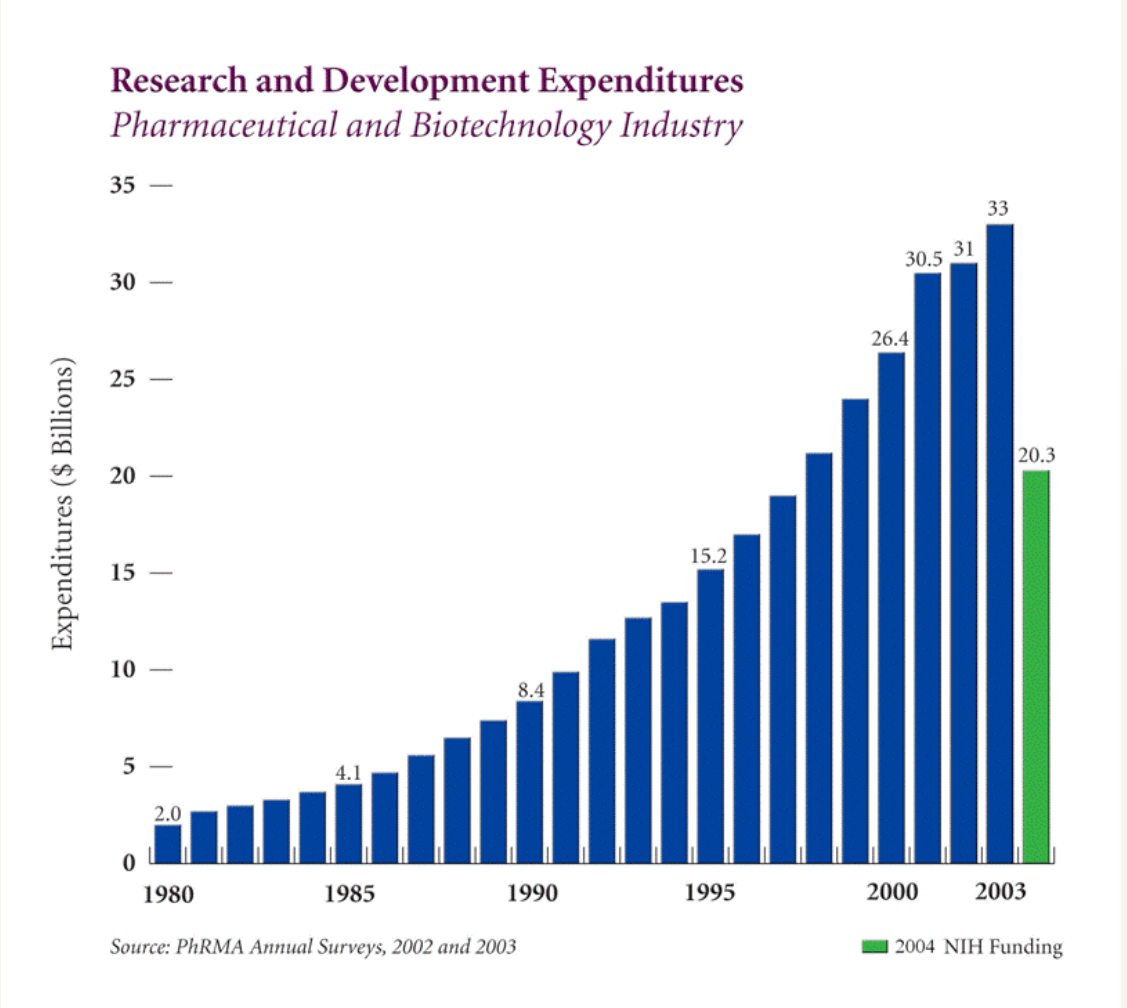

Limits to the Trial and Error Approach

Modeling and simulation is a way to learn more from the individual experiment, and to accumulate knowledge from experiment to experiment.

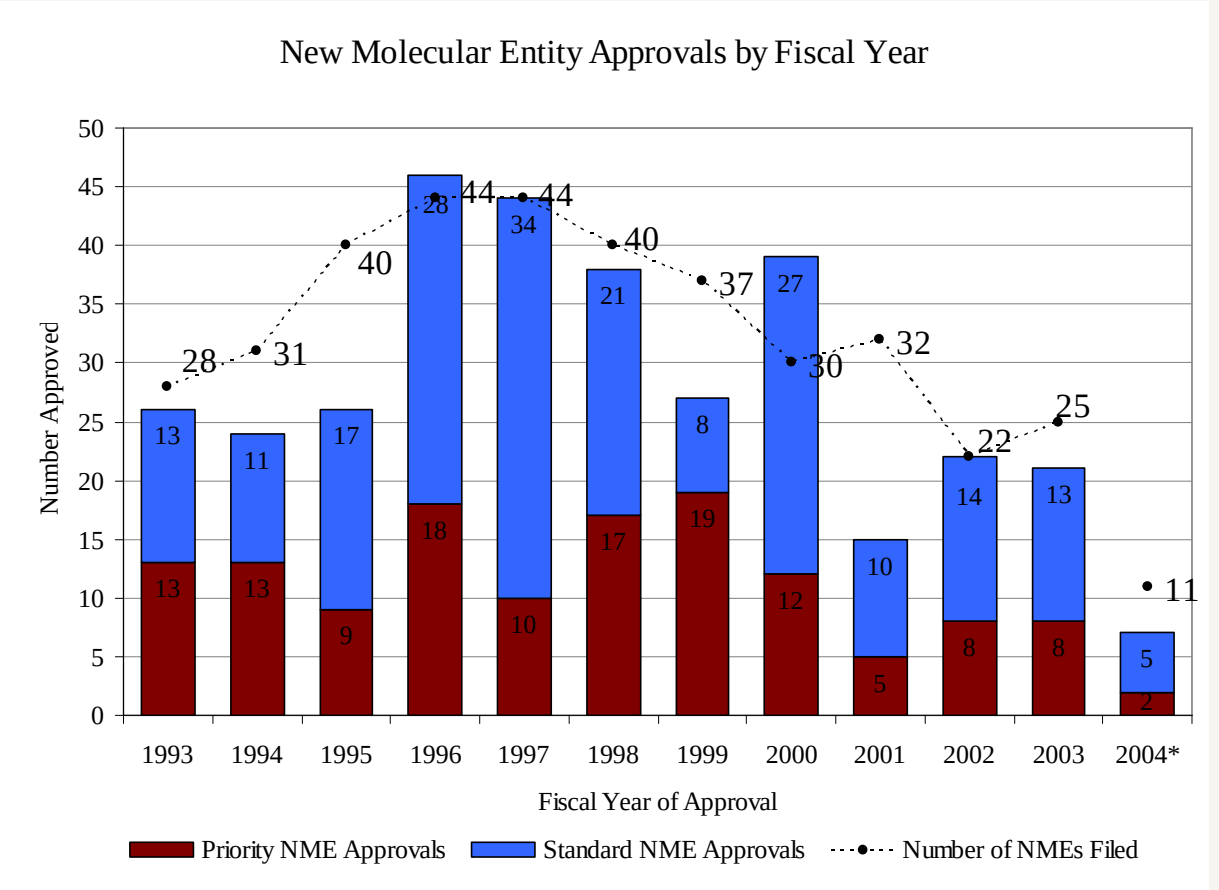

BioSim EU NETWORK OF EXCELLENCE

The Challenge to the Pharmaceutical Industry

The pharmaceutical industry is one of our best performing high-tech industries

- There are large and unmet needs for medical treatment, and patients justifiably expect new and effective drugs as an outcome of the widely announced breakthroughs in genomics and biotechnology.

- Despite a steady increase in R & D expenditures, the output in terms of new significant drugs has been steadily declining, and there are clear signs that the European pharmaceutical industry is falling behind its international competitors.

- Due to the large number of tests required to document biological function and prove the absence of adverse side effects, the development time is often as long as 8-11 years, and the development costs of a new drug run as hight as 800 mill Euro.

- 2 out of 3 drugs fail in the phase-3 trial because of toxicity or lack of efficacy.

- The traditional trial and error approach is no longer sufficient. The process should be based on a more directly on our understanding of the relevant biological processes.

A Rational Approach to Biomedical Research

The success we have had in the medical treatment of many diseases by far outstrips our understanding of the underlying biological and pathological processes

In mechanism-based modeling

- The relevant biological processes are represented as realistically as possible, and the parameters and nonlinear relations are determined through independent experiments.
- The model is initially validated by its ability to reproduce observed wave forms, frequencies, amplitudes, phase relationships, parameter dependences, and stability properties.
- Further validation of the model is based on its ability to predict the outcome of new experiments, performed under conditions not previously investigated.
- FDA strongly emphasizes the need for a simulation approach that can reduce the number of animal tests and provide a deeper understanding of drug functioning.

Subcutaneous Absorption of Soluble Insulin

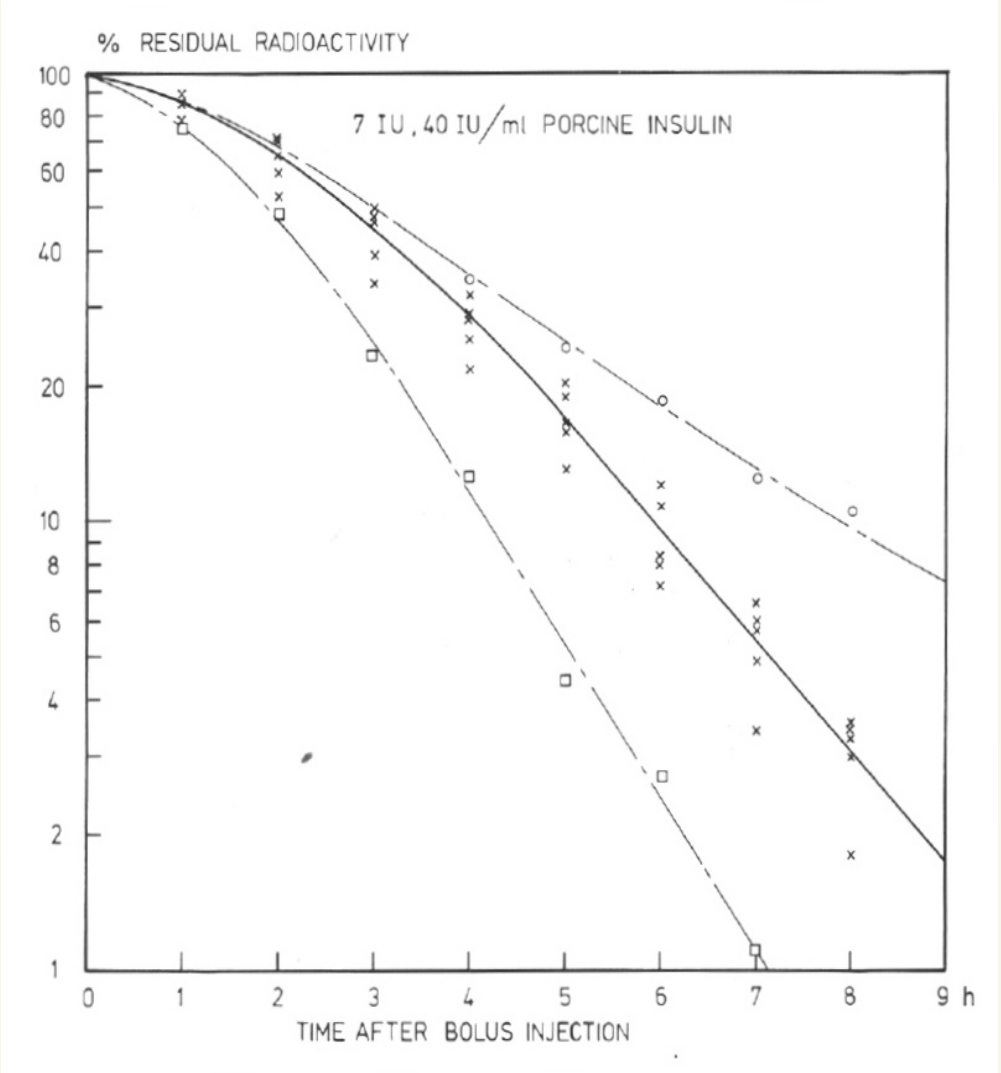

Absorption curves for 7 type-I diabetic patients following a bolus injection of 0.2 ml radio-labelled 40 IU/ml soluble insulin (Velosulin®).

The fraction of insulin remaining in the subcutaneous depot was measured over an 8h period.

Note the initial reduced absorption rate. This phenomenon can only be explained in terms of nonlinear mechanisms.

Collaborators

Christian Binder, Steno Memorial Hospital
Tue Søborg, Danish Medicines Agency and
Morten Colding-Jørgensen, Novo Nordisk

Absorption Curves for Different Dose Regimes

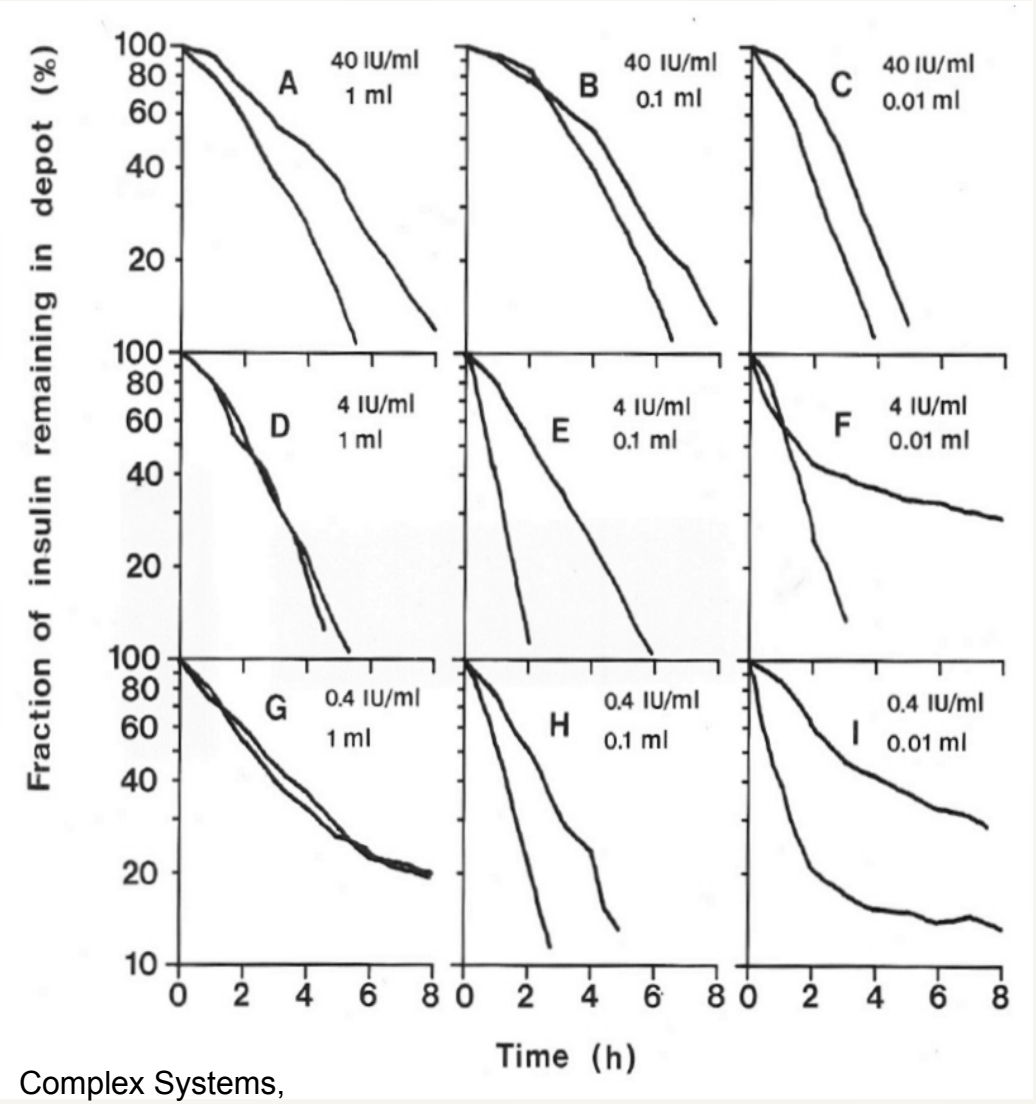

By performing experiments with different injection volumes and different insulin concentrations, one observes that:

There is both a volume and a concentration effect.

The delayed initial absorption is observed only for high volumes and high concentrations.

At low volumes and low concentrations a tail phenomenon develops.

Absorption Model of Soluble Insulin

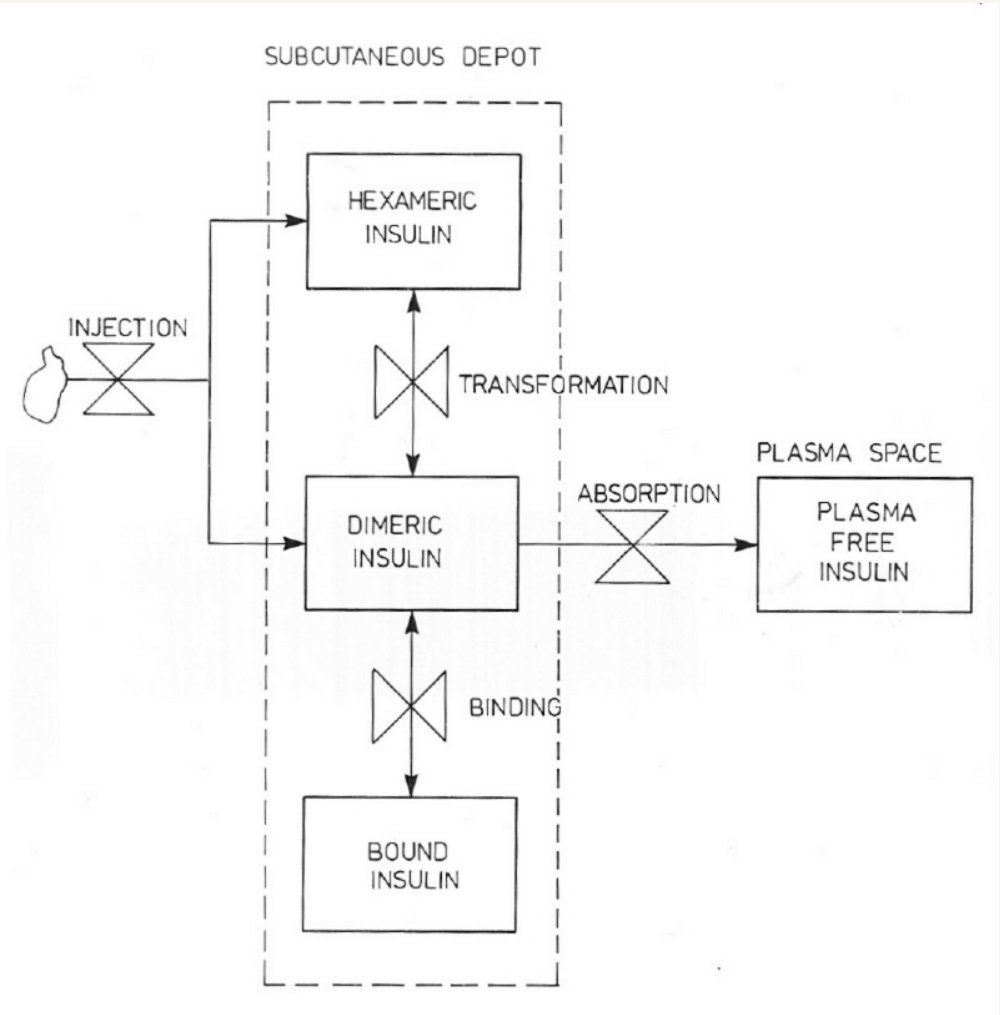

$$\frac{\partial C_H}{\partial t} = P(QC_D^3 - C_H) + D\nabla^2 C_H$$

$$\frac{\partial C_D}{\partial t} = -P(QC_D^3 - C_H) + D\nabla^2 C_D - BC_D - SC_D(C - C_B) + \frac{C_B}{T}$$

$$\frac{\partial C_B}{\partial t} = SC_D(C - C_B) - \frac{C_B}{T}$$

C_H, C_D and C_B represent the local concentrations of hexameric, dimeric, and bound insulin, respectively.

The terms $D\nabla^2 C_H$ and $D\nabla^2 C_D$ describe the rates of diffusion of the mobile insulin.

P and S are assumed to be large enough to establish quasiequilibrium.

Simulation Results

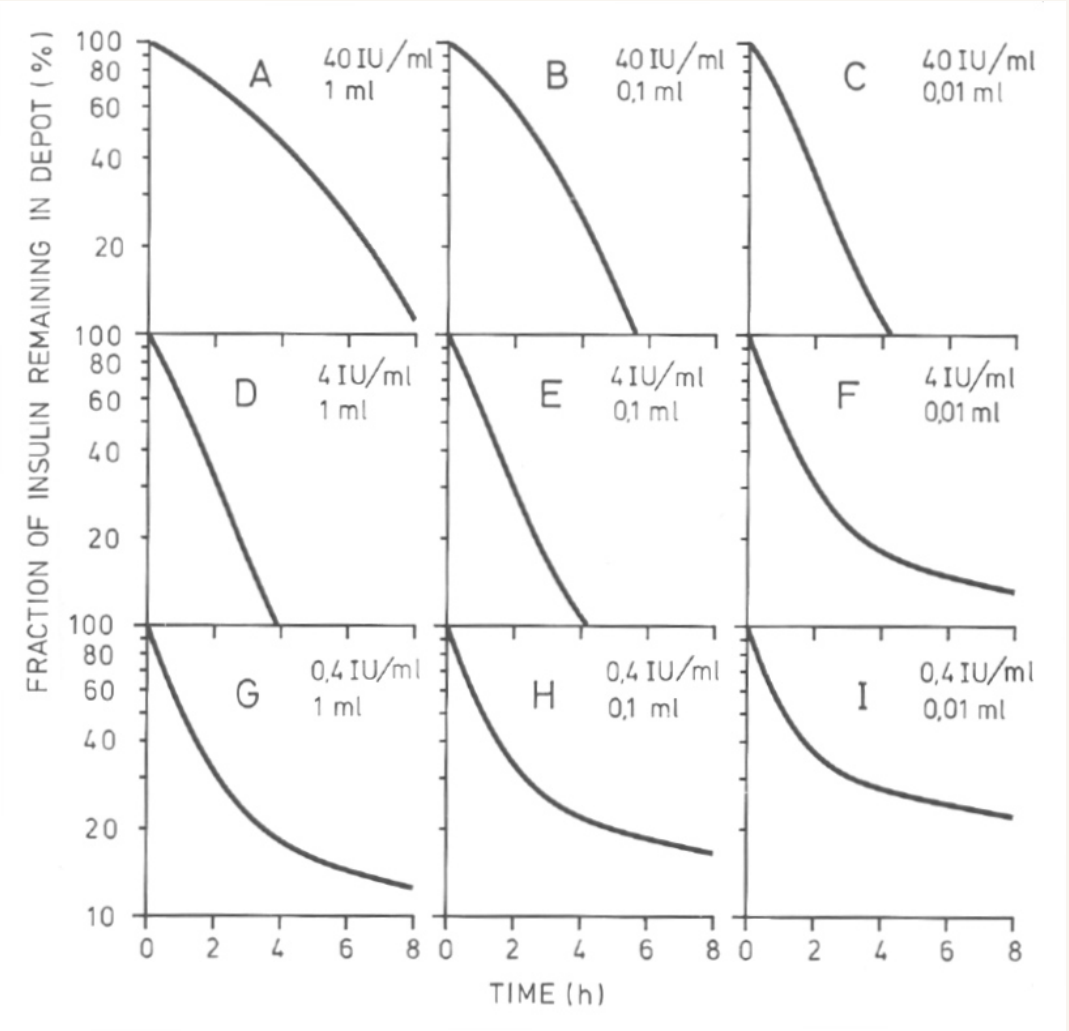

The model reproduces all the characteristic aspects of the observed absorption curves.

By fitting the model to individual features, one can determine the relevant parameters one by one:

For large volumes and large concentrations, the final slope determines the absorption constant *B*, and the initial slope determines the equilibrium constant *Q.*

The tail determines the concentration of binding states and the life time in these states.

Volume and Concentration Effects

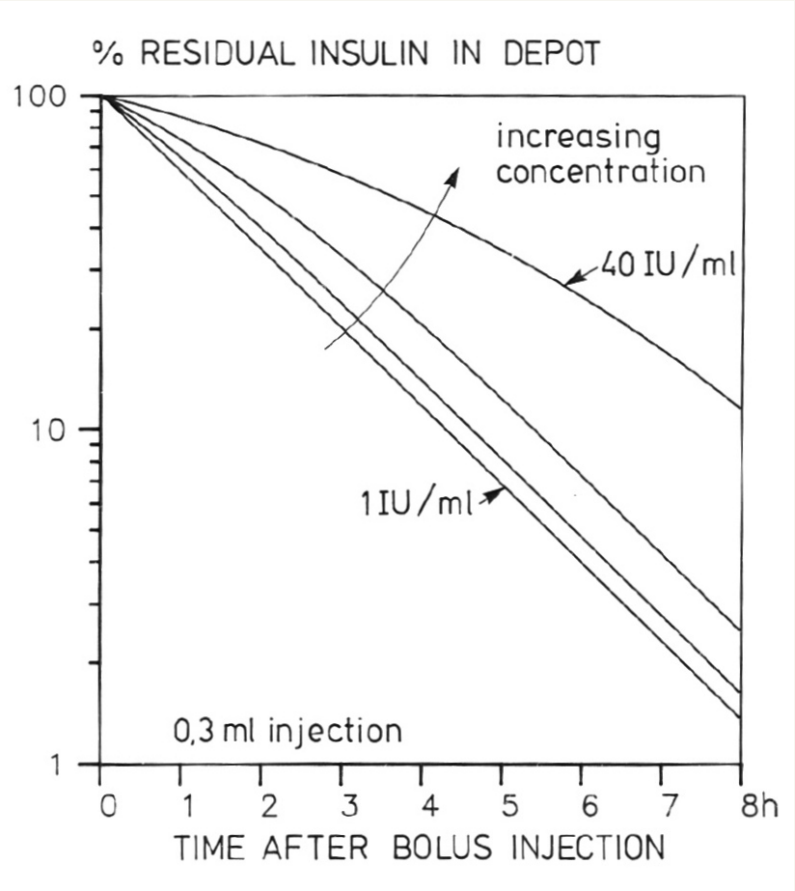

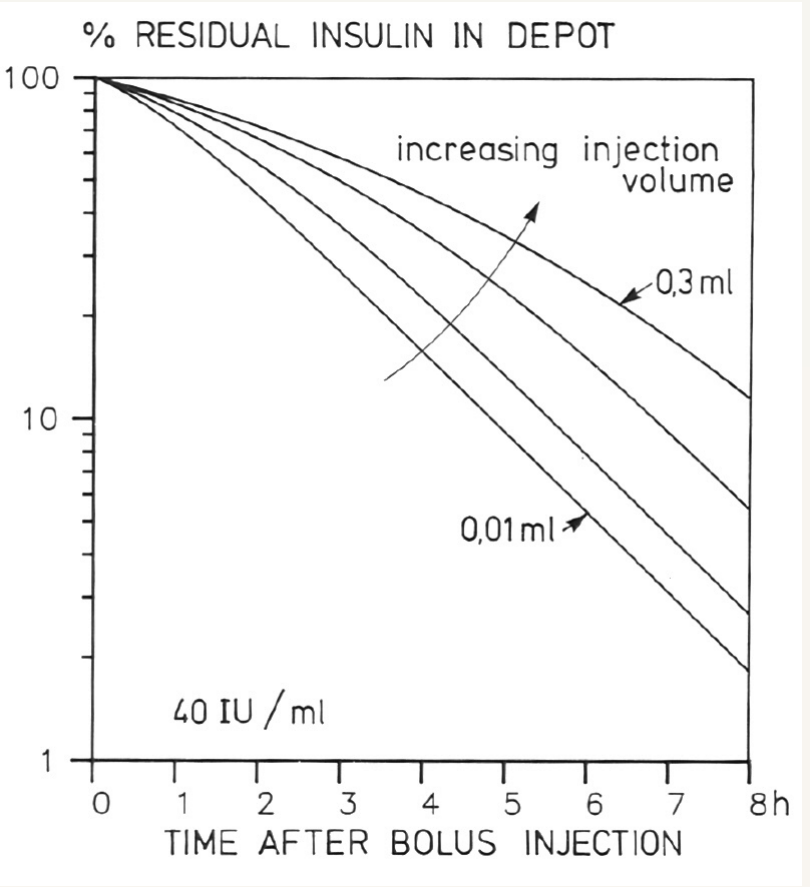

The model explains both the dependence on the insulin concentration and the dependence on the injected volume.

Fraction on Dimeric Form

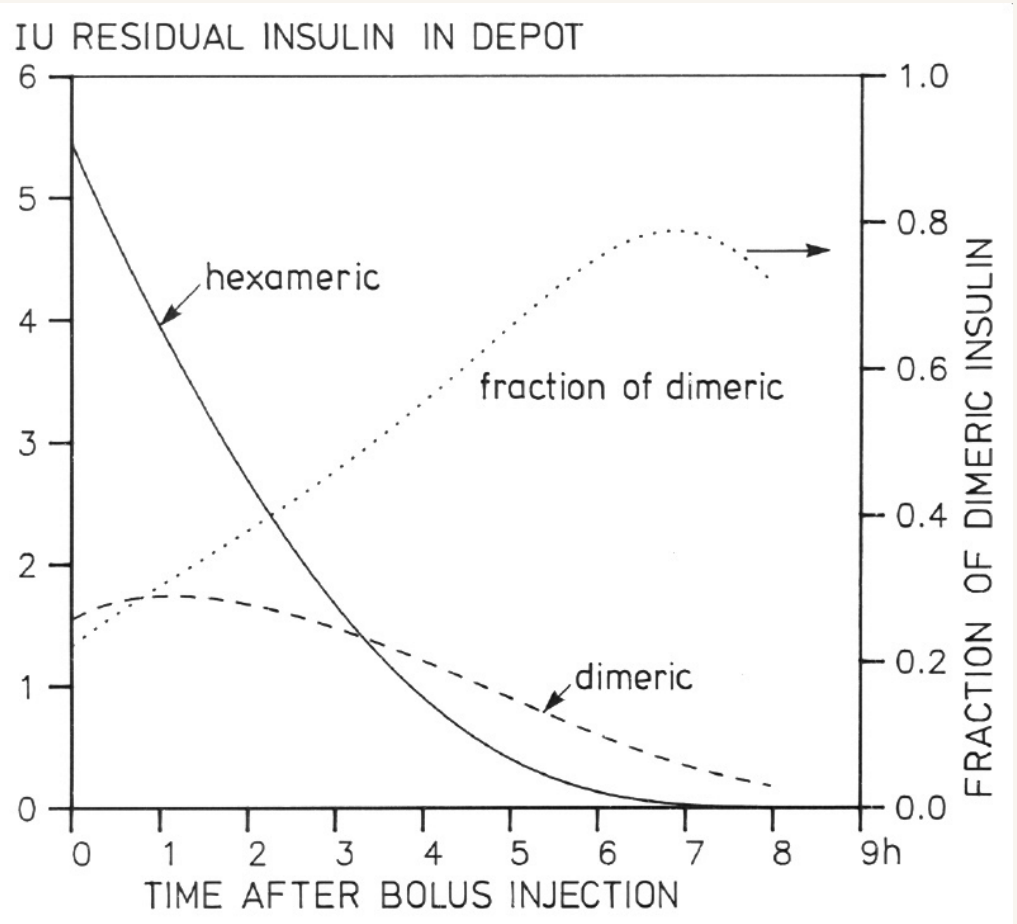

The model can be used to explain the individual variations of the three different concentrations and also, for instance, the fraction of dimeric insulin.

To the extent that these curves develop in an explainable manner, they provide an additional consistency check on the model.

We underestimate the absorption rate for dimeric insulin by approximately 30%.

Appearance Curves

The model has been extended by a plasma space and an extracellular space to describe the appearance of insulin the blood, diffusion into the extracellular volume and the associated rates of degradation.

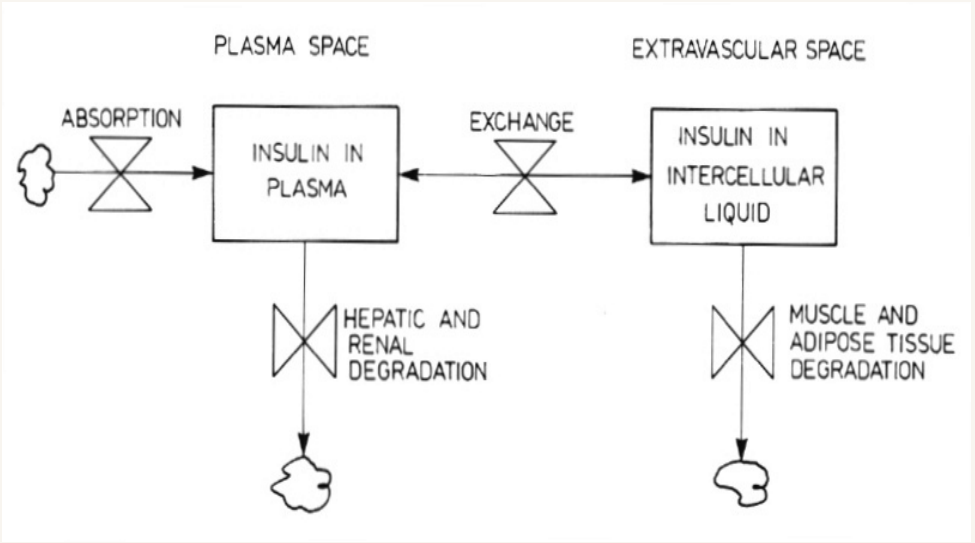

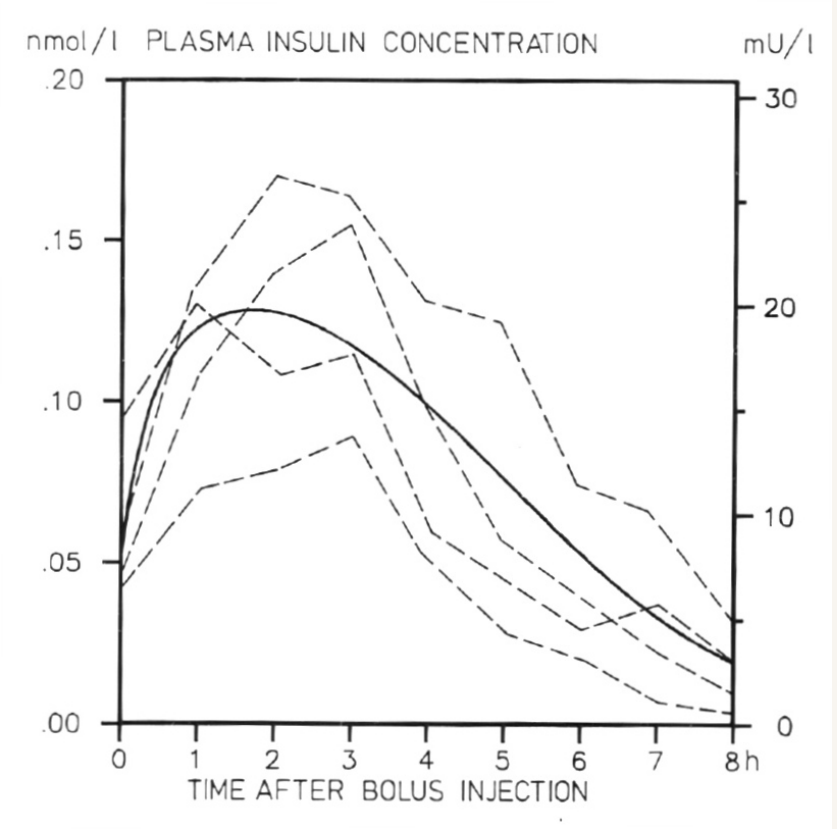

Can the model may now be used to simulate the outcome of experiments that have not yet been performed, e.g. the appearance rate for 100 IU/ml?

Recent Data for Insulin Appearance in the Blood

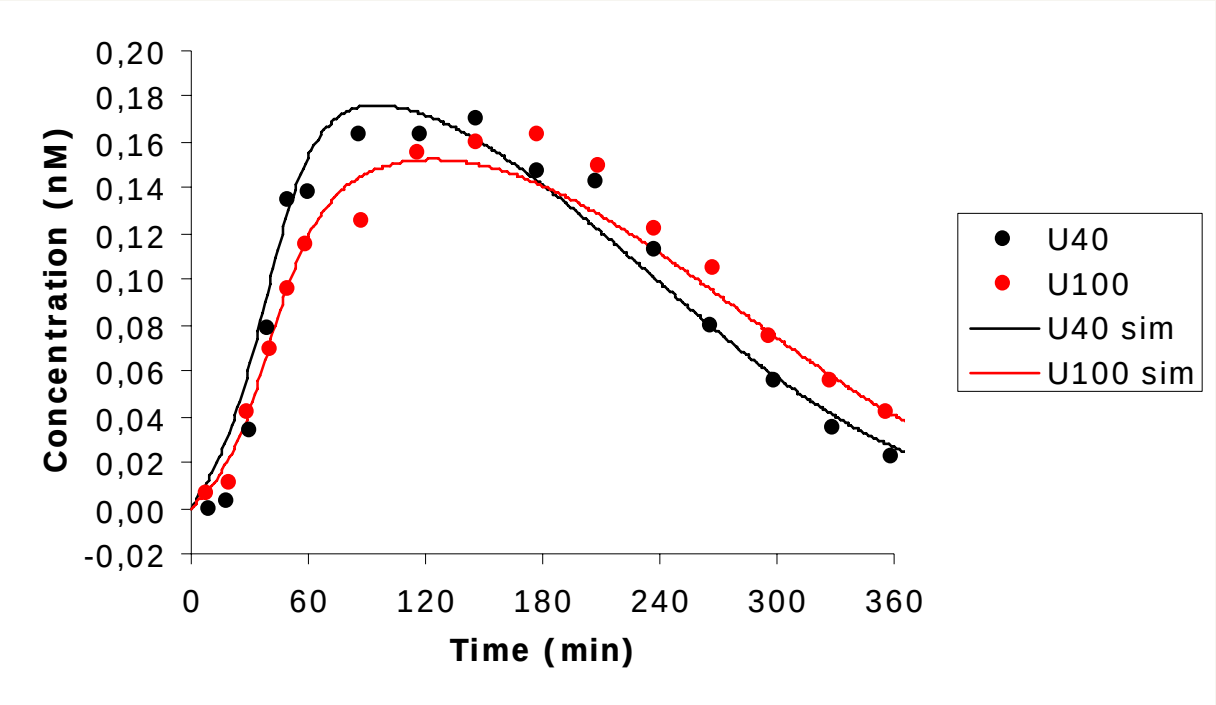

Experimental data (n = 6): 6 IU

With the same dose, one observes a delayed appearance in the plasma for higher insulin concentrations.

Simulations performed with the original parameter values.

As the injected insulin concentration increases, the delay in appearance becomes even more pronounced, and the maximum of the appearance curve is reduced. For higher insulin concentrations, one must expect the absorption delay to become very long.

May 2005

The Use of U-500 in Patients With Extreme Insulin Resistance

ELAINE COCHRAN, MSN, CRNP
CARLA MUSSO, MD
PHILLIP GORDEN, MD

ration of action of 5–7 h. U-500 has a pharmacokinetic profile more closely simulating NPH than regular U-100. U-500 insulin does not have anything added during its preparation to change its

insulin (10–14). These therapies seem to have their greatest role when the hyperglycemia is associated with obesity, as is the case with almost all type 2 diabetic

U-500 has a pharmacokinetic profile more closely simulating NPH than regular U-100.

NPH (Neutral Protamine Hagedorn) is a form of crystalline insulin.

Microdosing and the Criterion for Bioequivalence

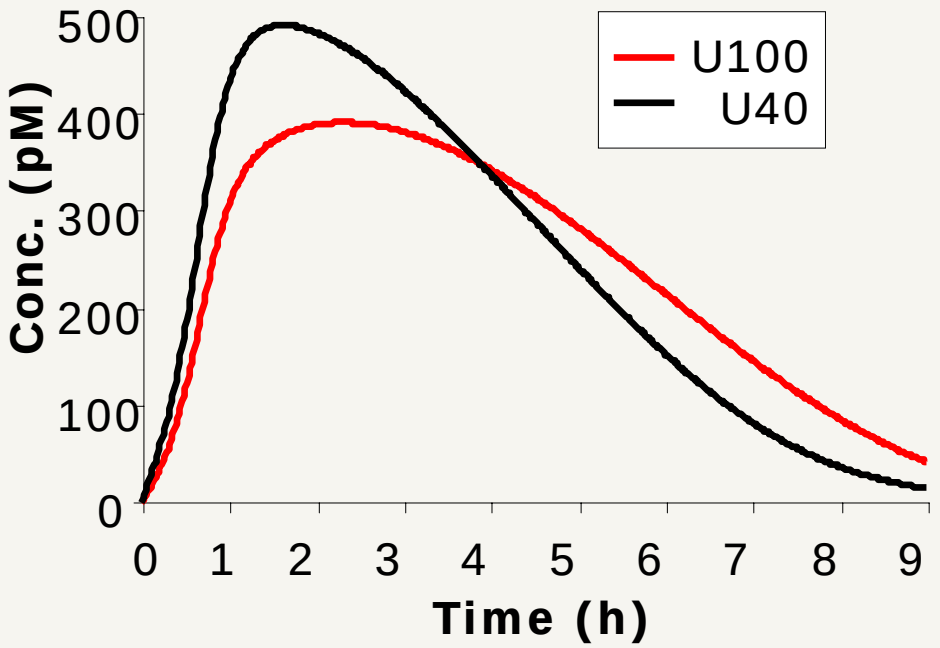

Simulation: 20 IU

There is no dose linearity, and there is no bioequivalence between the same dose administered with different concentrations.

The area under the curve is the same for the two simulations. However, the ratio of the C_{max}-values is (slightly) larger than the factor 1.25 accepted by the European Medicines Agency (EMA).

The idea of microdosing is to reduce the number of animal experiments by 'going into man' at an earlier stage in the drug development process using initial doses that are thousand times smaller than the anticipated active dose.

Slow Acting Crystalline Insulin

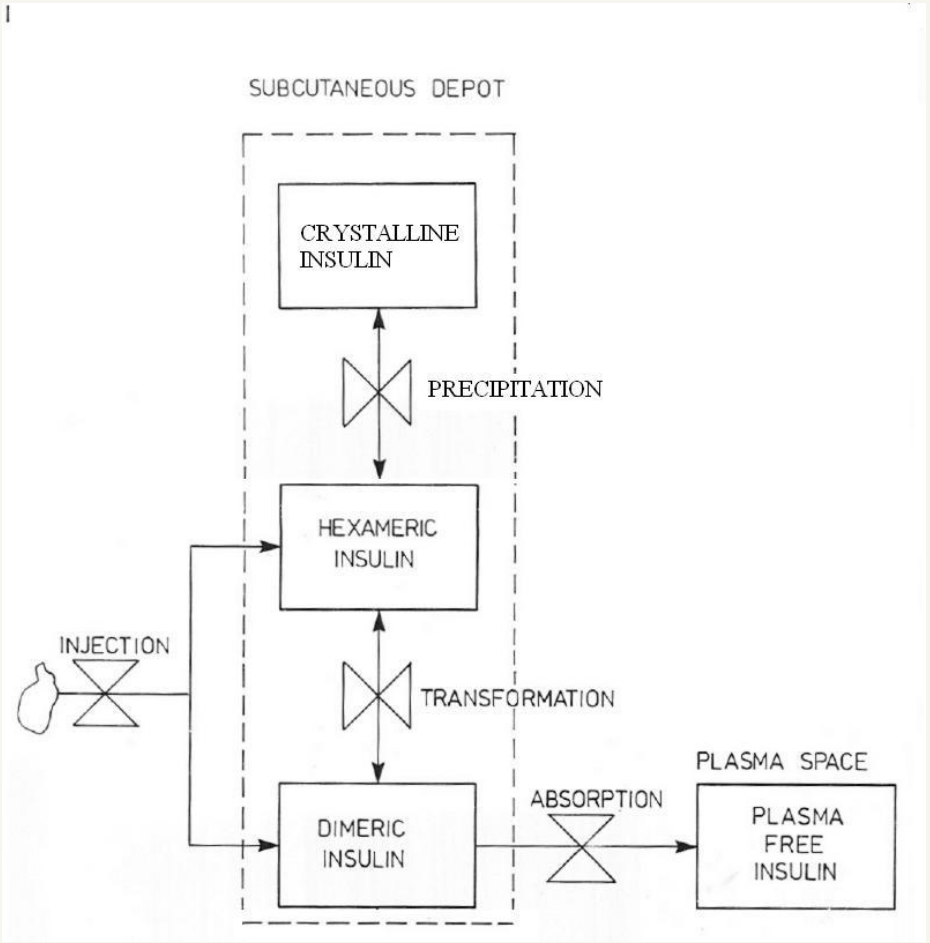

Insulin variants in crystalline form are used with both Zn and protamine as precipitation promoters.

These formulations have a much slower absorption rate than soluble insulin and are used as base treatment with
2-3 injections per day.

We must know the processes and rate constants that control dissolution and precipitation.

Addition of Zn or protamine may also affect the dimeric/hexameric balance. Hence, we must know, how fast these additives disappear from the injection site.

Absorption of Crystalline Insulin

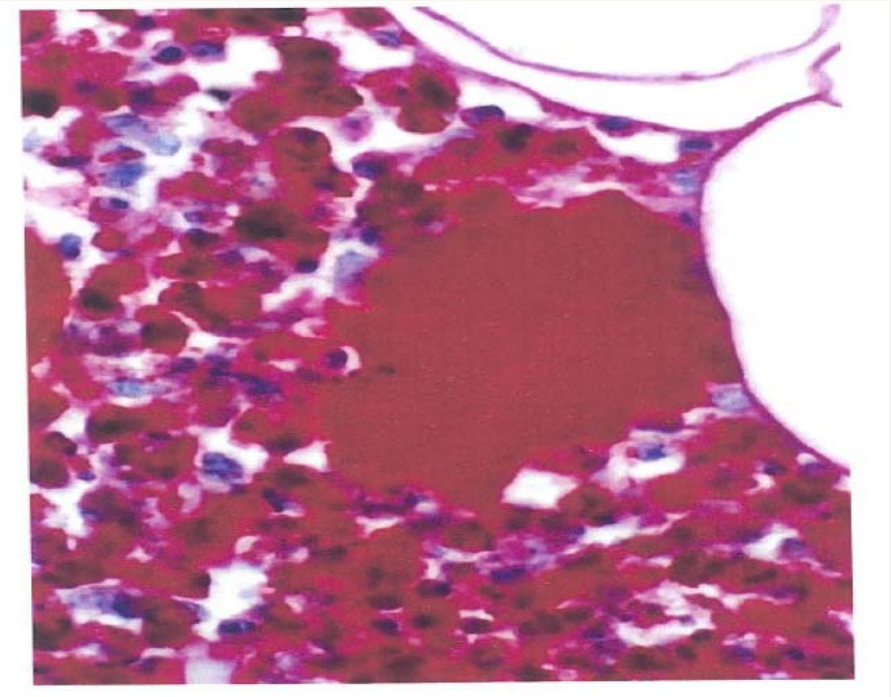

Additional equations:

$$\frac{dC_{NPH}}{dt} = -\beta C_{NPH}(1-\alpha C_H C_P) - A_{NPH} C_{NPH}$$

$$\frac{dC_P}{dt} = \beta C_{NPH}(1-\alpha C_H C_P) + B_P C_P + D_P \nabla^2 C_P - A_P C_P$$

Insulin crystals (red) between fat cells (white) in adipose tissue. Insulin decomposition partly takes place via attacks on the crystals by macrophages (violet).

Conclusion:
Different insulin formulations involve different mechanisms and require different model structures.

Variations in Blood Flow

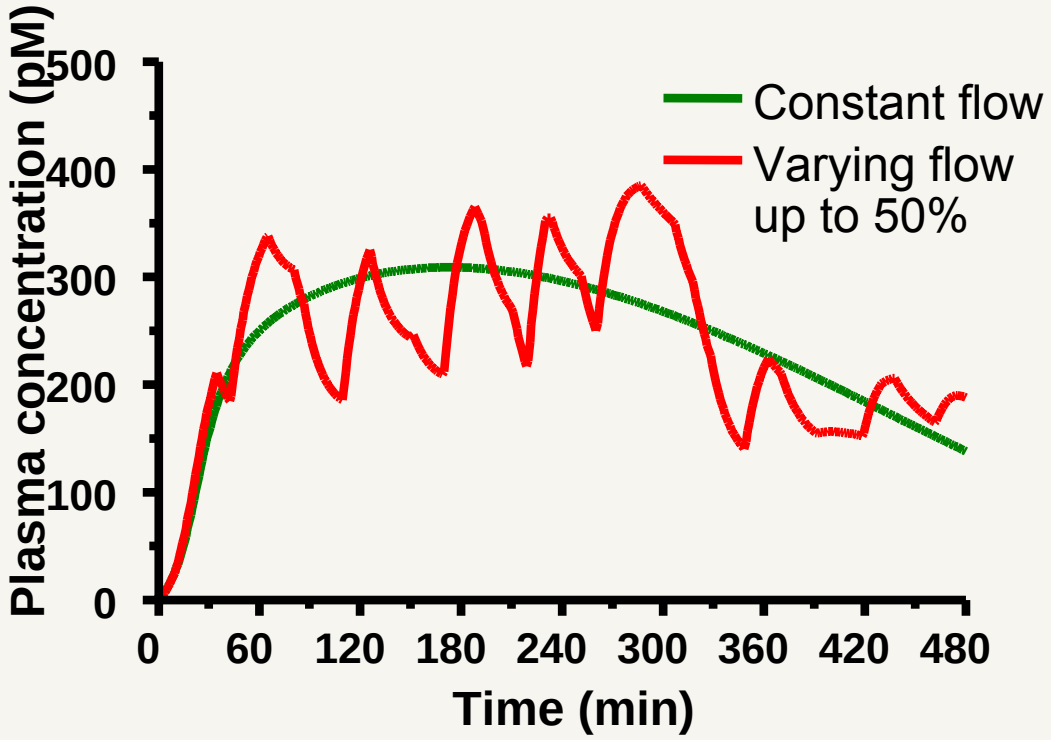

Variation in the blood flow at the injection site can cause significant variations in the rate of insulin appearance, particularly if the blood perfusion is low (obesity, reduced skin temperature, meals, etc.).

This phenomenon can be modelled by inserting an additional compartment in the model to describe the amount of insulin in the local capillary blood volume.

C_{max} and $T(C_{max})$ are no longer well-defined from the experimental traces.

A possible way to reduce the significance of blood flow variations could be to use an insulin formulation that binds to some protein (albumin) in the blood.

Absorption Model for Albumin Bound Insulin

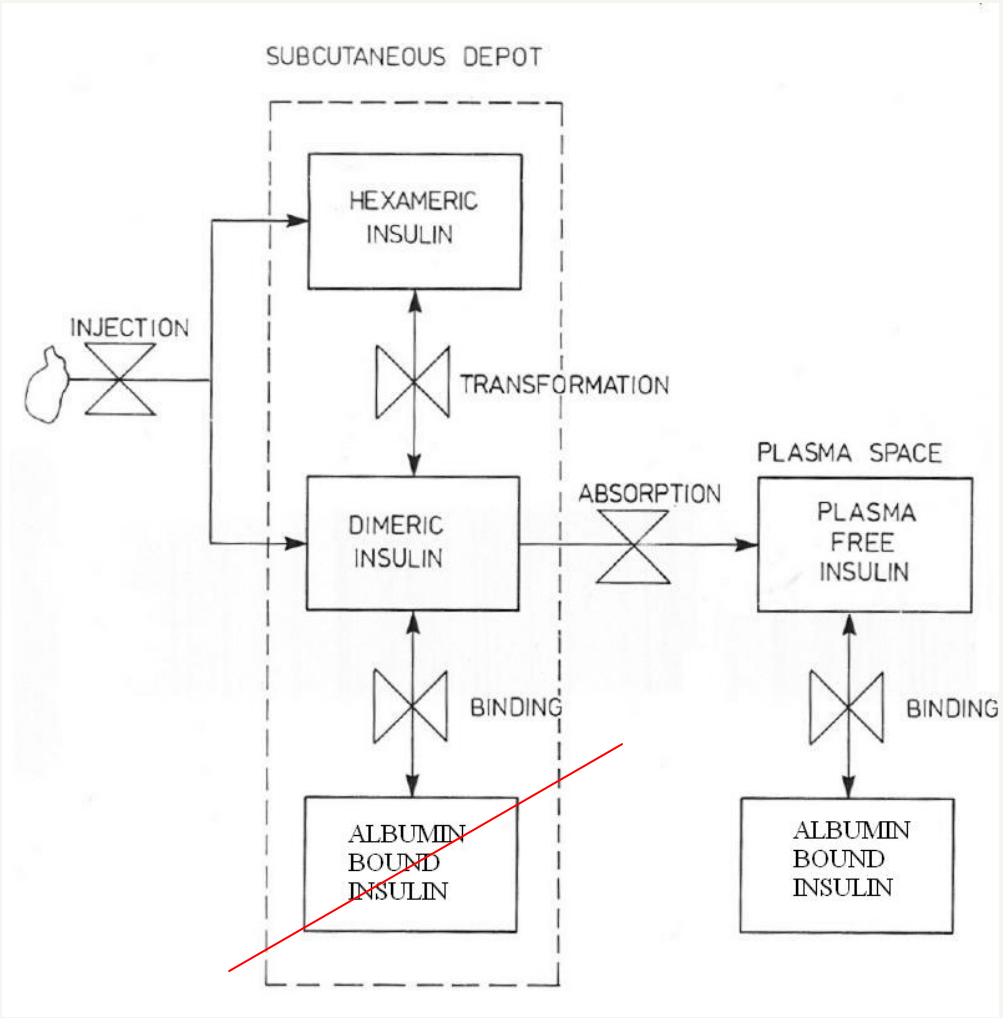

The idea is to generate a pool of bound insulin in the blood from which free insulin can be released at a well-defined rate.

We must know the albumin concentration in the blood and the reaction rate constants for the formation and dissociation of the insulin-albumin complex.

The model can then predict the time profiles of free and albumin bound insulin in the blood, and we can examine the response to fluctuations in peripheral blood flow.

Basic Mechanisms of Insulin-Glucose Regulation

Boxes represent amounts of either glucose or insulin in a specific compartment.

Full lines denote material flows, and dotted curves represent causal relations.

The model is equivalent to three coupled differential equations of the general form:

$$\frac{dI}{dt} = \text{insulin secretion} - \text{insulin degradation}$$

$$\frac{dG}{dt} = \text{glucose uptake} - \text{glucose consumption}$$

Normal insulin production 1200 mU/h and normal extracellular glucose concentrations 900 mg/l.

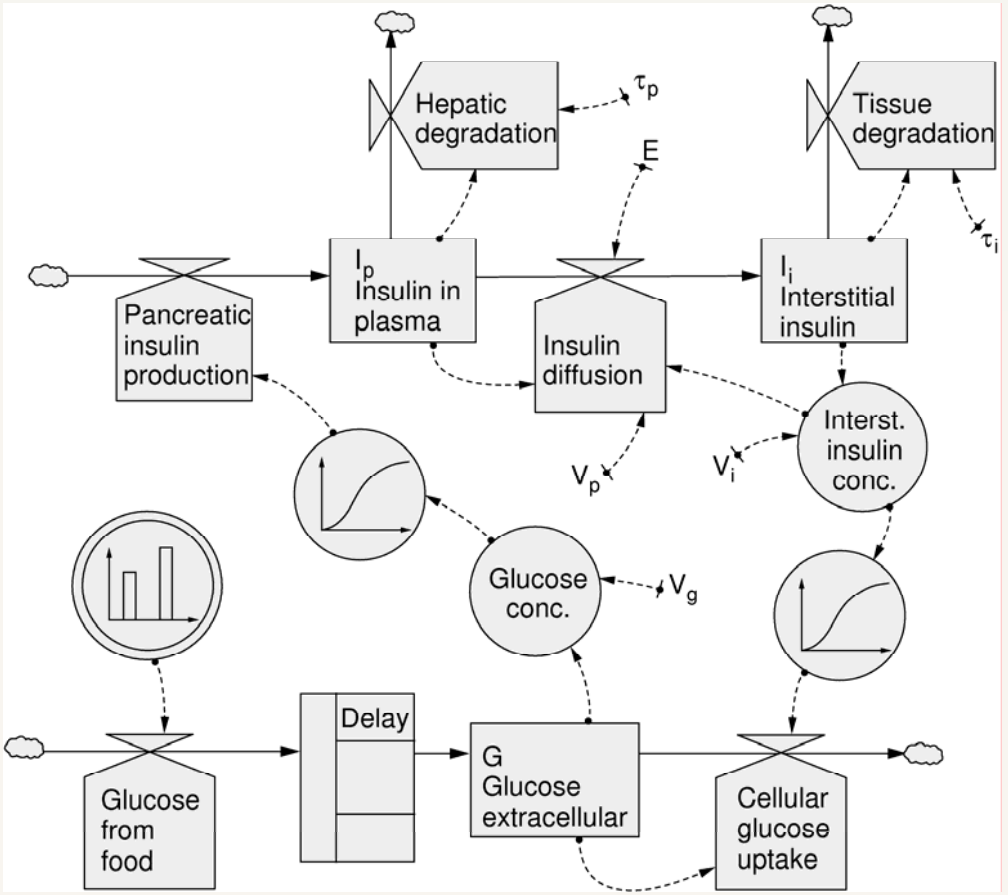

Simulating the Response to a Series of Meals

The timing of the meals and their volumes in terms of equivalent glucose contents are specified exogenously.

For the healthy person, the increase in blood glucose is accompanied by a rapid increase plasma insulin concentration.

By virtue of the nonlinear character of the model, the response to a given meal depends of its timing and size relative to previous meals.

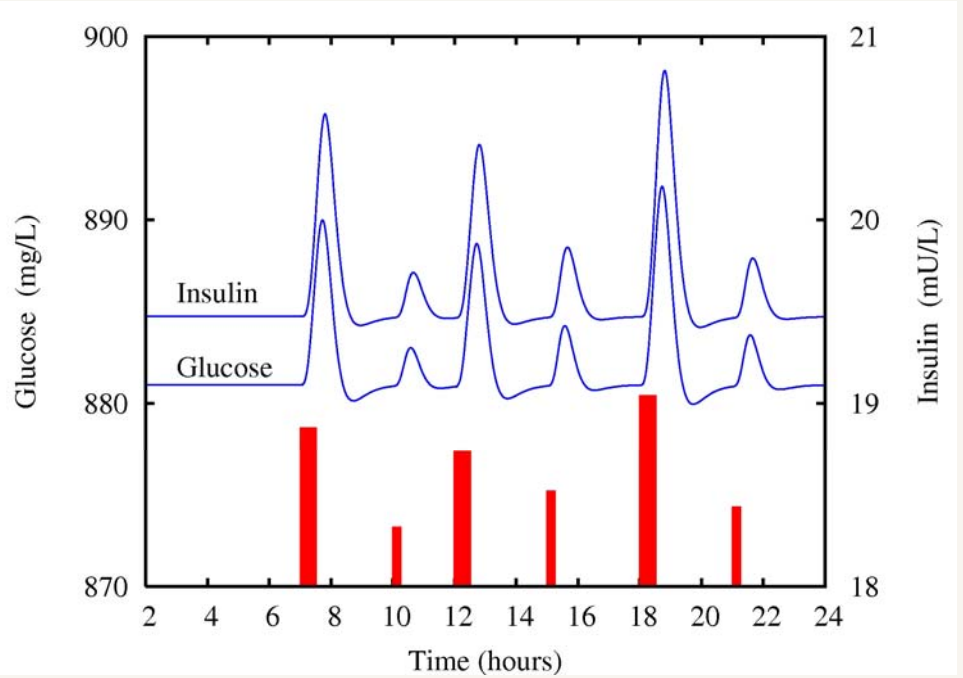

With appropriate extensions,accounting e.g. for the role of other metabolic substances (fat, protein, keton bodies, etc.), the model may be used to simulate more advanced issues of the metabolic control system.

Simulating Insulin Pump Operation

The objective of replacing insulin bolus injections by smaller, more frequent infusions from an insulin pump is to maintain a more constant and better regulated plasma insulin concentration.

Considering that the life time of insulin in the blood is as short as 6 min, a basic question is how high the pump rate needs to be.

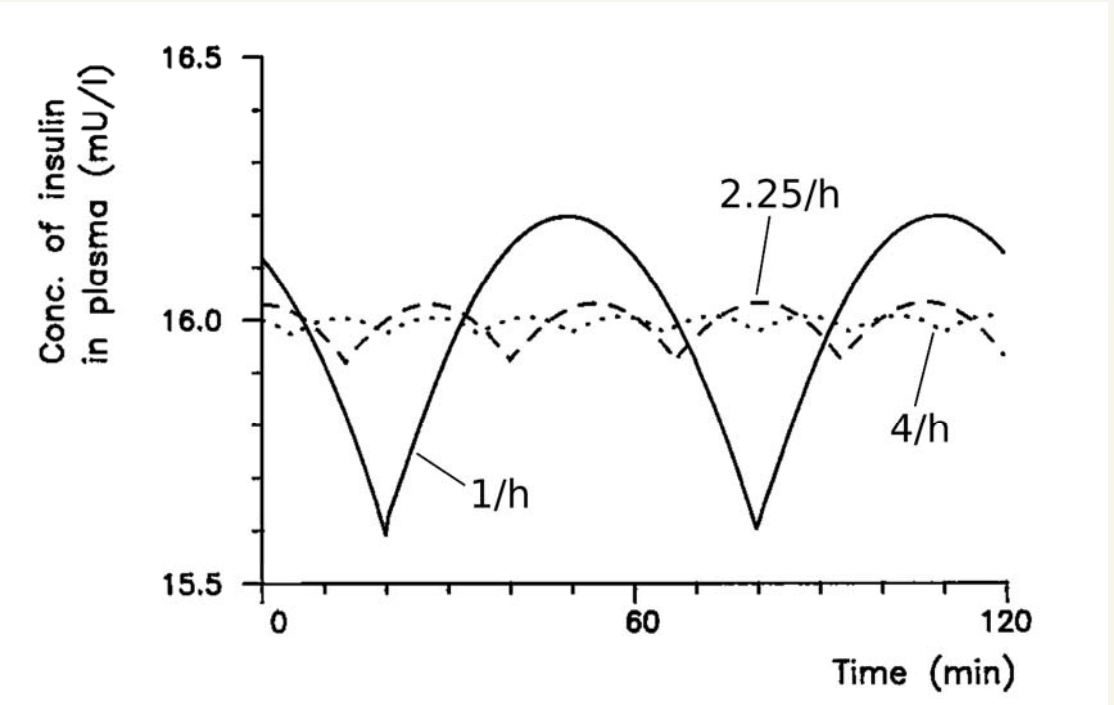

Our calculations show that, due to the build-up of a depot in the subcutaneous tissue, a pump rate of one infusion per hour suffices to keep variations in blood insulin concentration associated with the finite pump rate below 3%

Bone Structure

The interior of the vertebral bodies and other large bones consists of a complex network of plates, columns and struts with diameters varying from 10 to 400 μm.

One can calculate the strain-stress relation for such a structure by means of the type of computer programs that were used many years ago to design railway bridges.

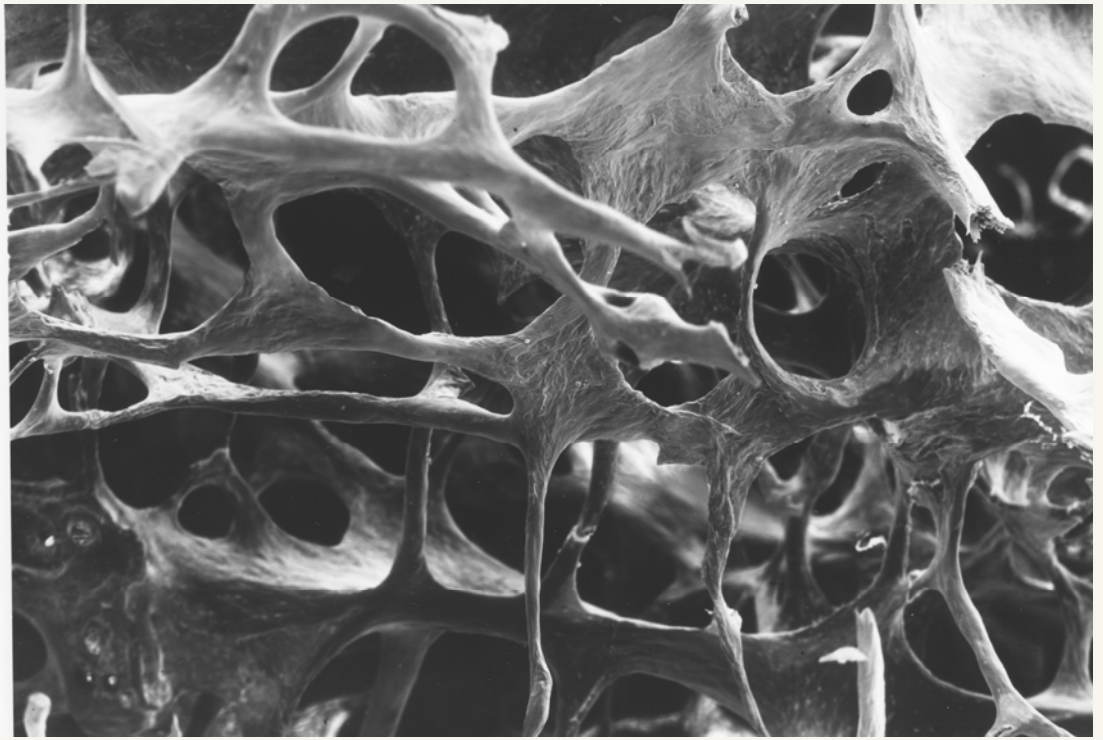

This allows us to determine the bone strength in terms of parameters such as the material properties of the individual trabecula, its form (diameter and length), the regularity of the structure, and the density of the network.

With Lis Mosekilde and Jesper Skovhus Thomsen, Aarhus University

Bone Remodeling

Like other materials subject to repetitive loading, bone is liable to fatigue failure. However, bone tissue is capable of self-repairing.

This repair (bone remodeling) occurs at discrete sites that may be active for 4-8 months and thereafter rest for 2-5 years.

During the menopause the structural changes are accelerated and presumably accompanied by an increase resorption depth.

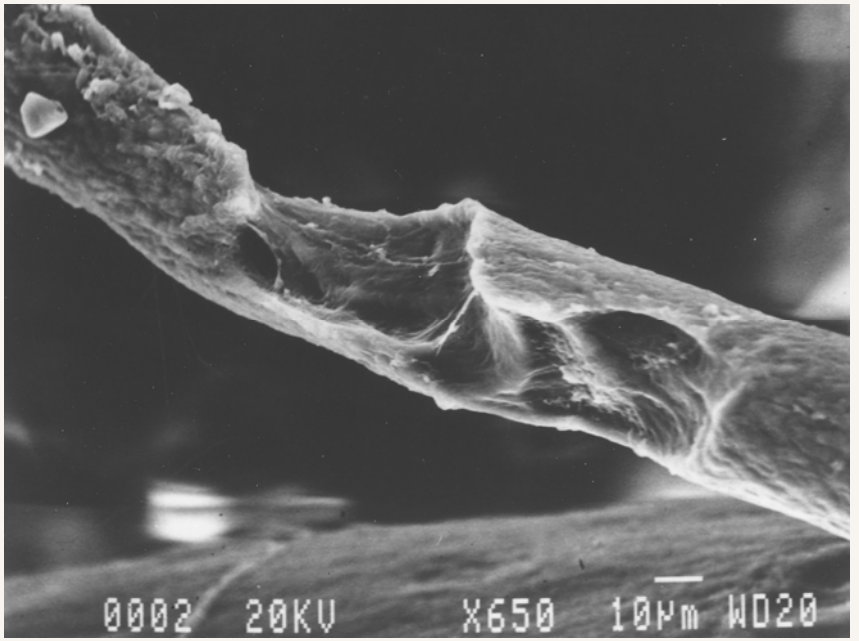

Activation of a site is initiated by a resorption phase during which osteoclasts engulf bone tissue (collagen fibers and minerals). The rate of activation depends on biomechanical requirements, age and sex as well as on a number of hormonal and nutritional factors.

Different Phases of Bone Remodeling

Through gap-junction coupling, the original bone forming cells (osteocytes) maintain a communication network.

This network appears able to be able to sense piezoelectric signals and is likely to play a major role in controlling the remodeling process.

The resorption phase leaves a rough surface with 50-60 μm deep lacuna. In the adult person, resorption is coupled to a formation process in which osteoblasts deposit fresh bone material.

Snapshots of the process can be obtained from bone biopsies.

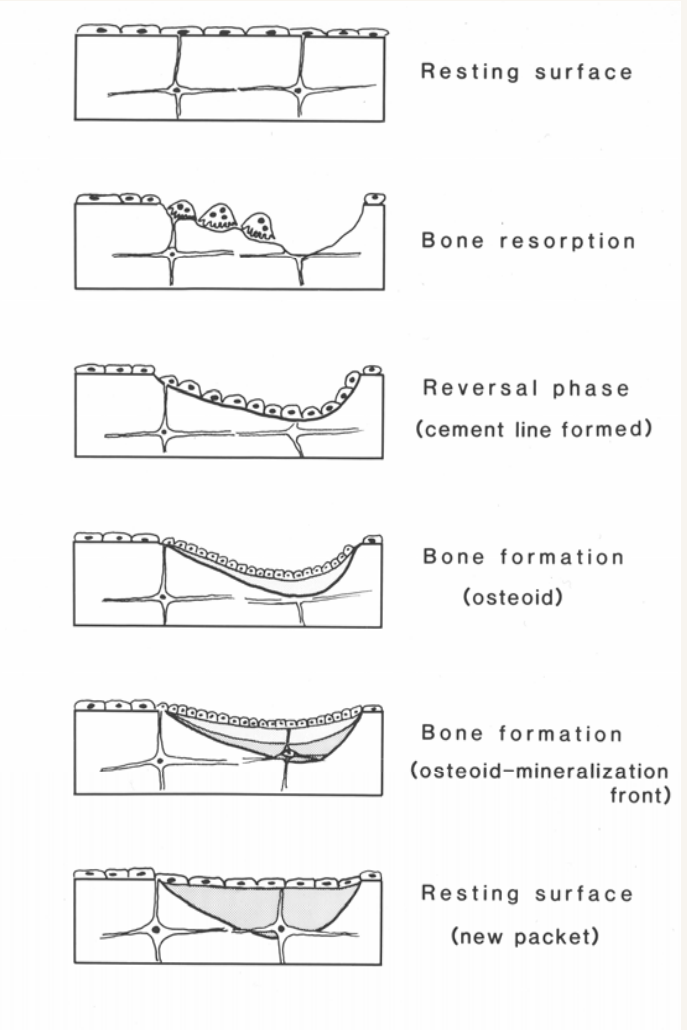

Trabecular Strength and Perforation Rates

Remodeling usually gives rise to a net loss of bone mass.

By means of a stochastic model one can simulate variations in the trabecular diameter and rates of perforation in terms of the

initial diameter
critical thickness
activation frequency
resorption depth and area
formation balance, etc.

accounting, e.g., for effects of immobilization, life in space, the menopause and various medical treatments.

Simulations of the menopause for two different activation frequencies and two different resorption depths.

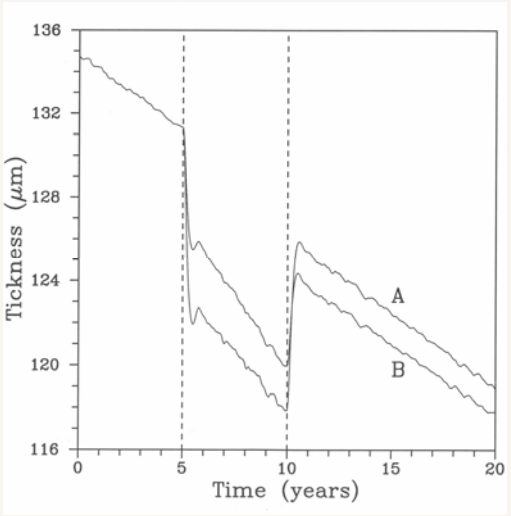

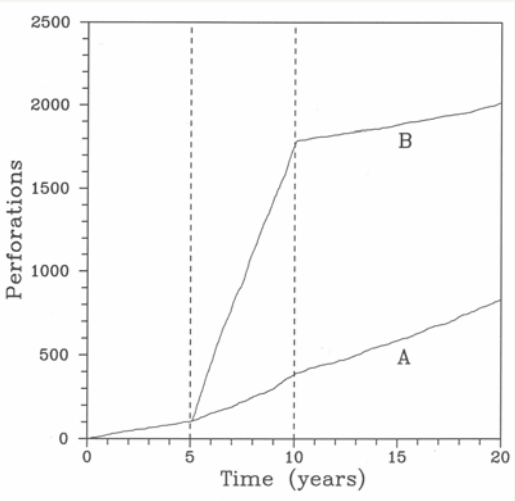

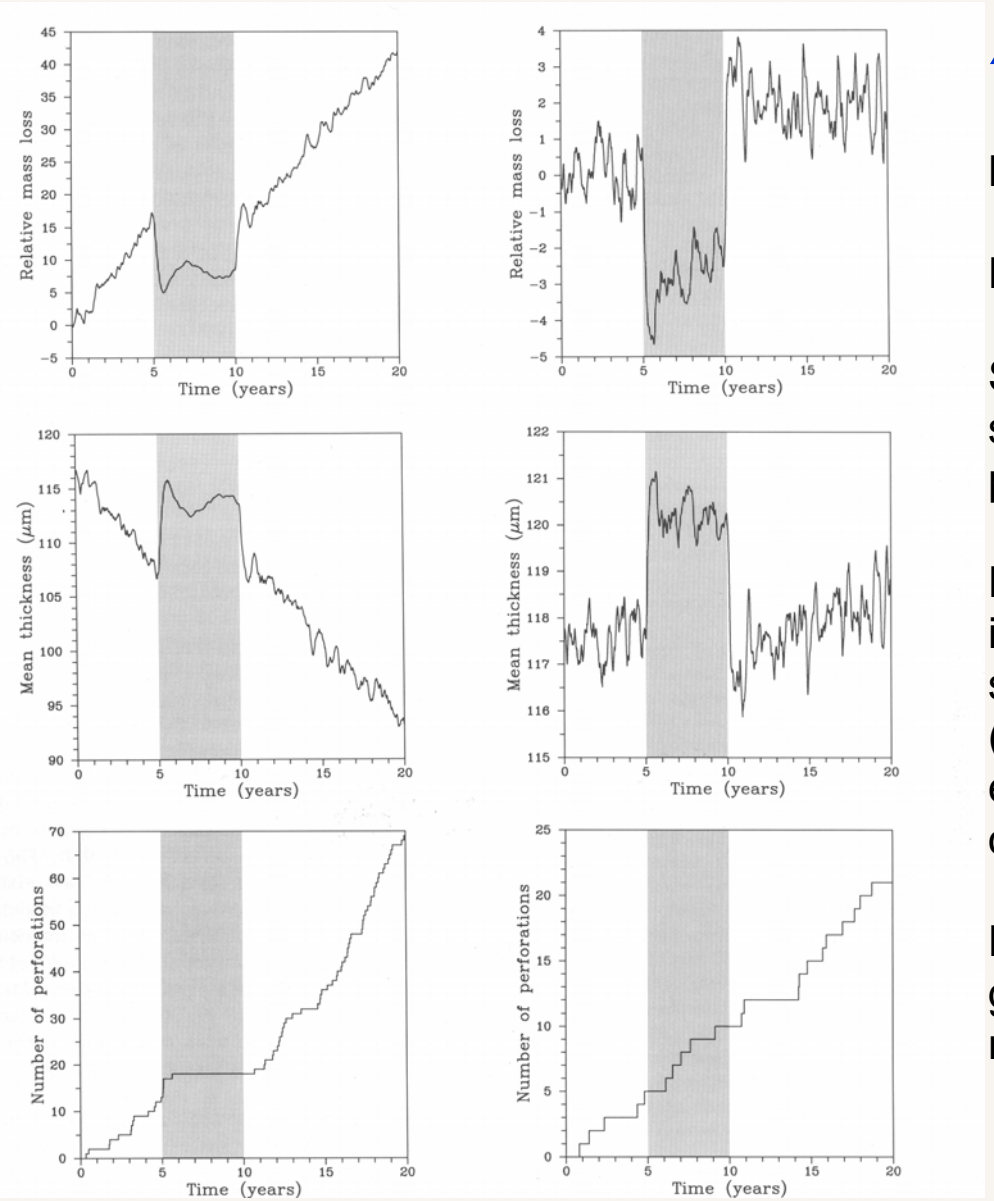

Antiresorptive treatment

Left: Etidronate treatment

Right: Estrogen treatment

Simulations are initiated at age 60. Gray shaded areas represent the treatment period.

Etidronate and estrogen both cause a slight increase in bone mass, and Etidronate also seems capable of preventing perforations. (Simulation of fluoride therapy indicates an even more effective reduction of the number of perforations).

Relative mass loss is bone mass lost at a given time in percentage of initial bone mass.

Loss of Bone Strength with Age

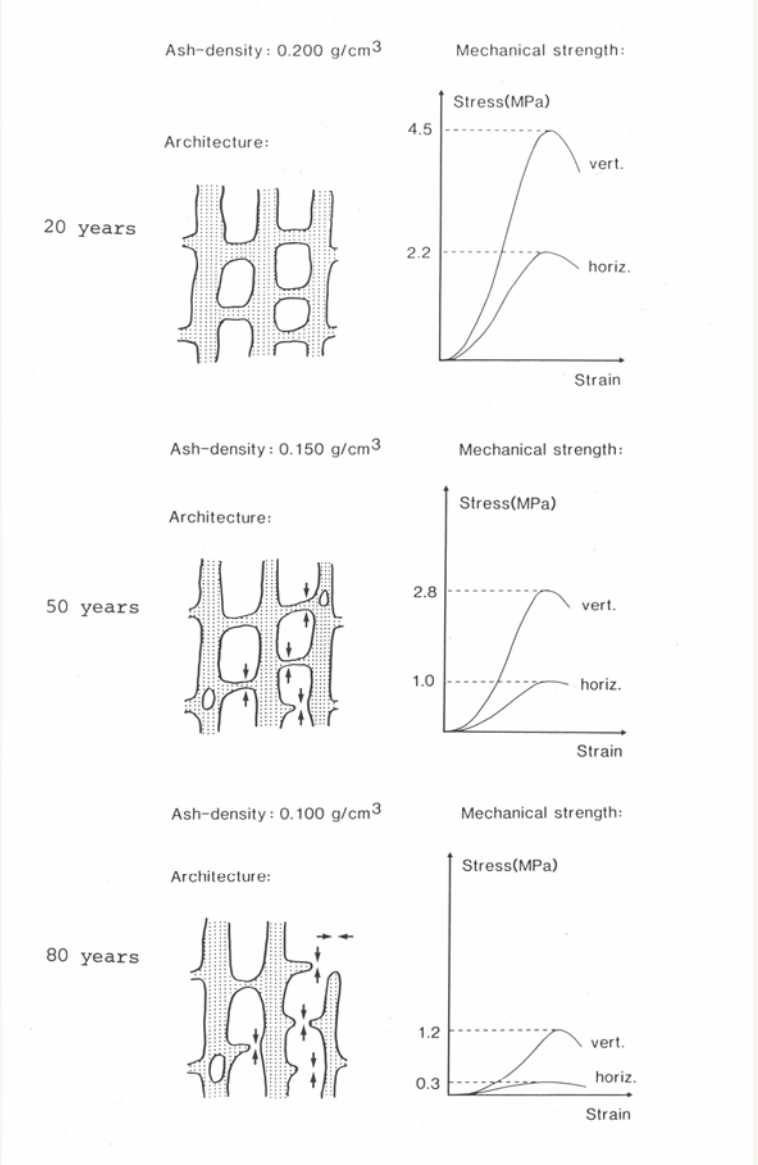

By combining the remodeling process with the structural model we can describe the development of bone strength with age.

While the loss of bone mass is two fold from the age of 20 to 80 years, the concomitant loss of strength is four fold.

The model integrates the consequences of a large number of informations obtained on the microscopic level into useful predictions on the macroscopic level.

The model allows us to investigate the effect of different assumptions regarding the microscopic and structural parameters and to relate the predictions to personal characteristics.

The Systems Approach: Close the Loop

The most characteristic feature of living organisms is their system's nature as reflected in the large number of interacting feedback mechanisms that regulate the biological processes at different length and time scales.

An effective application of modeling can improve the treatment of many diseases, lower the development time and costs for new, effective drugs and reduce the need for animal experiments.

As more information becomes available, data-driven methods must yield to methods that allow data to be interpreted directly in the context of already existing knowledge.

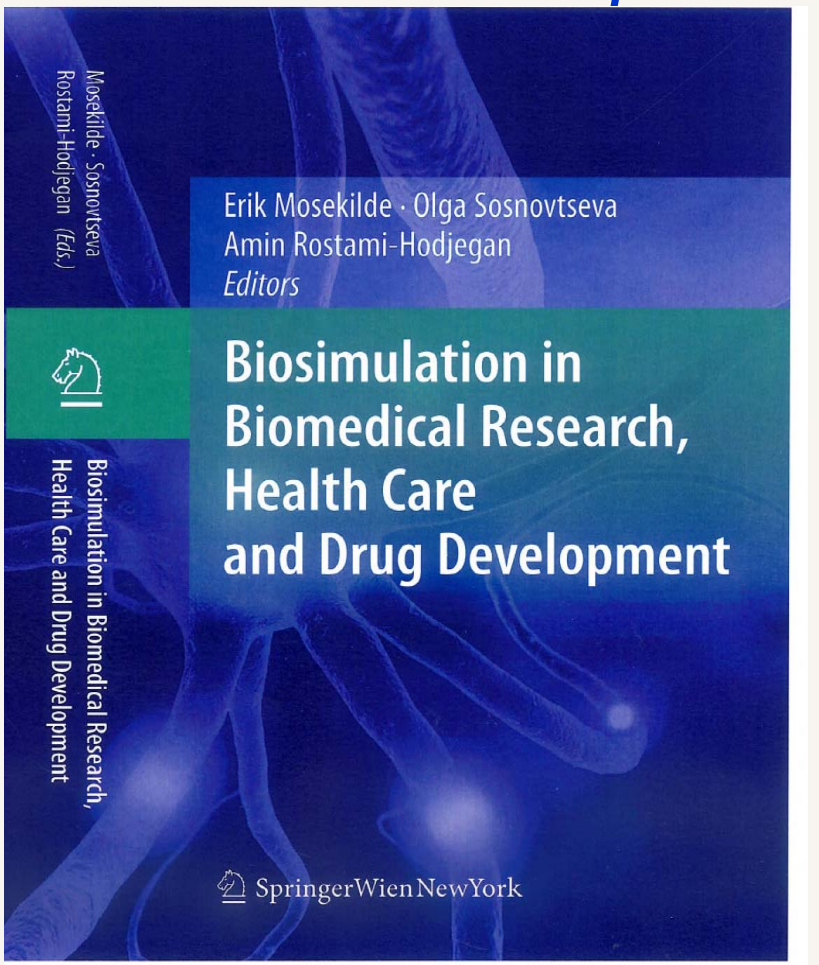

Modeling and simulation has been used for many years in most other industries, and the result has always been enormous savings in development time and costs.

BioSim
EU NETWORK OF EXCELLENCE

Complex Biomedical Systems

1. Modeling and Simulation in Biomedical Research and Health Care
2. *Role of Nonlinear Dynamic Phenomena in Living Systems*
3. Synchronization and Chaos in Nephron Autoregulation
4. Bifurcation Structures in Interacting Biological Units
5. Exercises

DTU

The 24 Hour Circadian Rhythm

❖ The individual cells of the body dispose of a circadian timing system through which a network of core genes controls the transcription and inhibition of various regulatory compounds.

❖ The cellular clocks are synchronized by hypothalamic pacemaker signals, and this allows the circadian rhythm to coherently modulate cellular activity (i), body temperature (ii), cortisol (iii) and melatonin (iv) secretion, etc.

❖ In particular, the circadian timing system modulates both cellular proliferation rates and the metabolism of many drugs.

❖ As demonstrated by *Levi et al*., this effect is strong enough for an eight hour shift in administration time to produce an eightfold increase in the tolerability of more than 30 anti-cancer drugs.

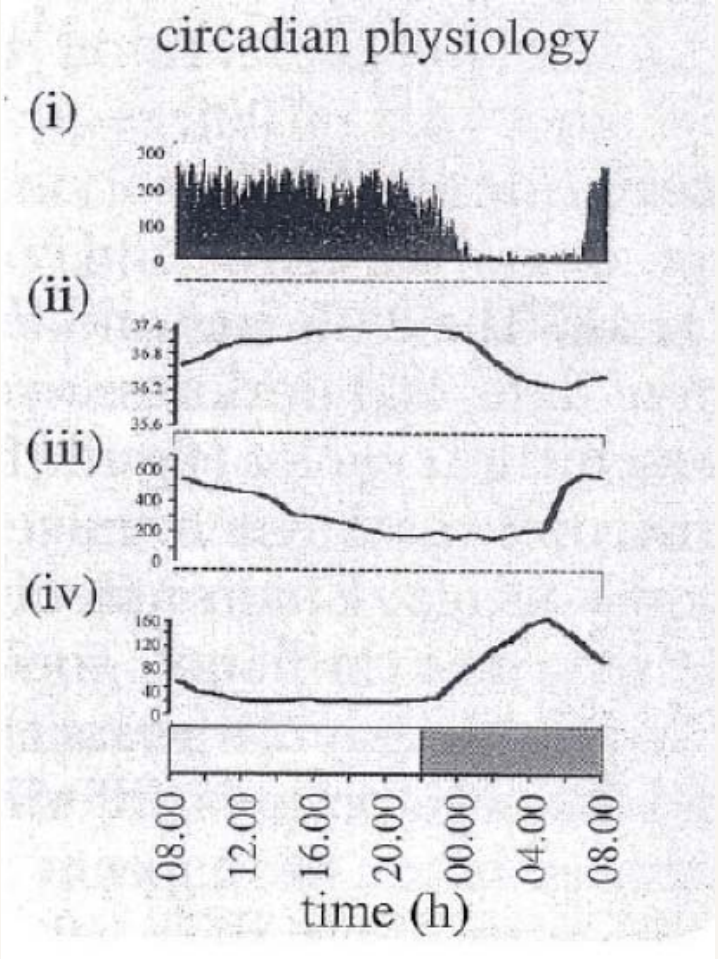

24 Hour Growth Hormone Profile

Some hormones (e.g. luteinizing hormone and testosterone) are released in a regular train of pulses with 2-3 hour intervals.

Other hormones exhibit a more irregular pattern, and the question arises to what extent this can be given a deterministic explanation associated, for instance, with the interaction between several pulsatile systems.

A strongly varying hormone concentration may be more efficient than a constant concentration with the same average value.

Moreover, in the presence of such patterns, the time of administration of a drug may be significant. This is exploited, e.g. in connection with the treatment of cancer, but may be significant in many other diseases as well.

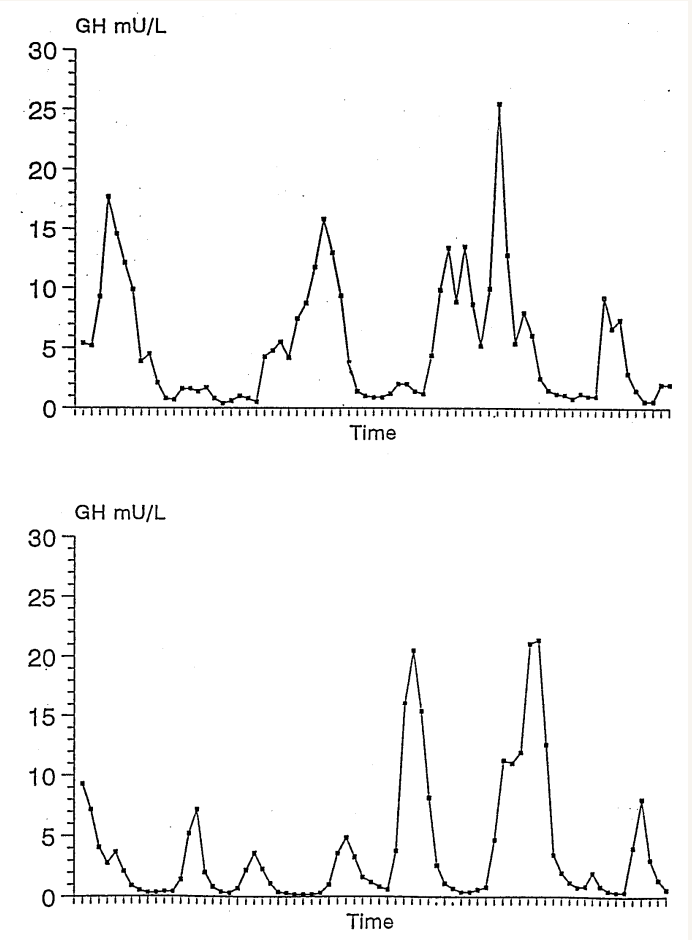

Bursting and Spiking Pancreatic Beta-cells

- Isolated beta-cells tend to produce randomly looking spike sequences in their membrane potentials.
- Intact cells in pancreatic islets produce bursts of spikes with a bursting fraction that varies with the glucose concentration
- Insulin is released during the bursting period. Isolated cells typically release insulin at significantly lower rates than islet cells.
- The bursting dynamics arises from the interaction between a fast potassium dynamics and a slower calcium dynamics. The electrophysiological processes again couple to metabolic oscillations in the cell.

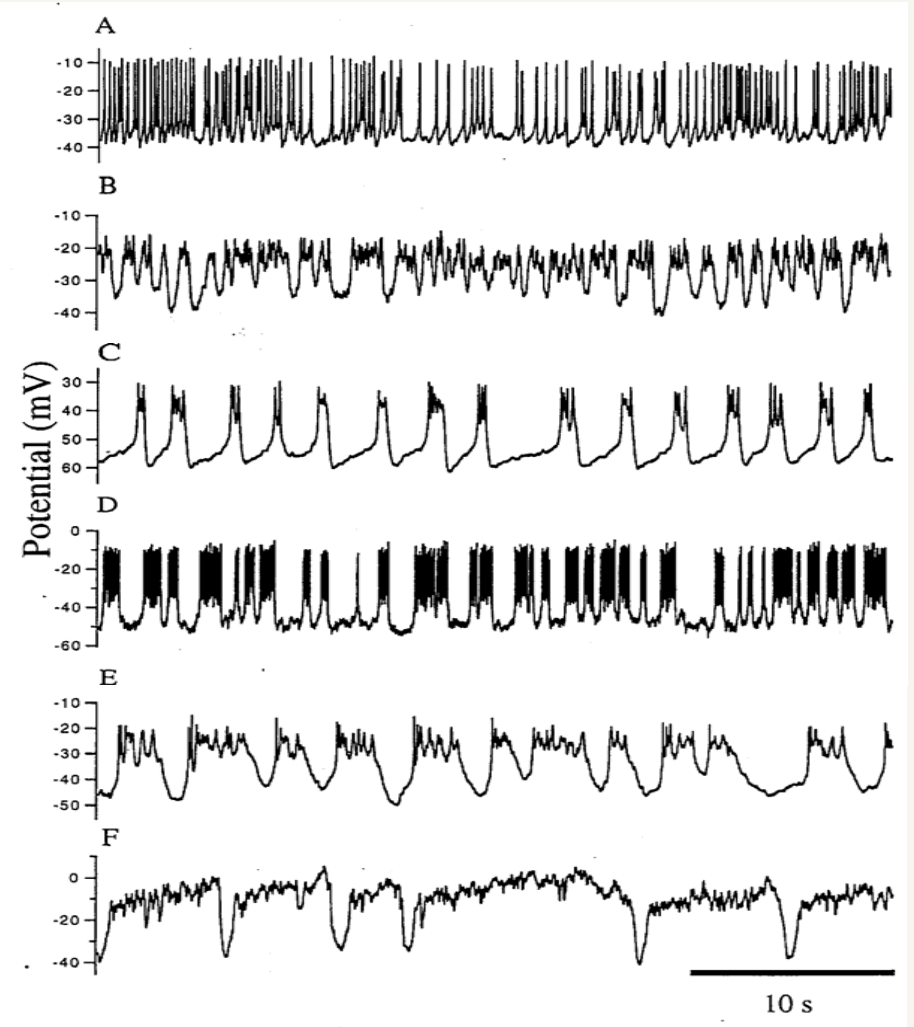

Synchronization of Neighboring Cells

Two beta-cells can synchronize both their bursting and their spiking behavior, even if they are not particularly close to one another in an islet of Langerhans.

The beta-cells interact via gap-junctions, via variations in the intercellular ionic concentrations, and via local insulin and glucose concentrations.

Activation of smooth muscle cells (e.g., in the arteriolar walls) similarly involves synchronization of the cellular oscillations in the cytosolic Ca^{2+} concentrations.

Several diseases (such as Parkinsonian tremor, epilepsy, depression, heart failure, etc.) involve a malfunctioning interaction among the cells.

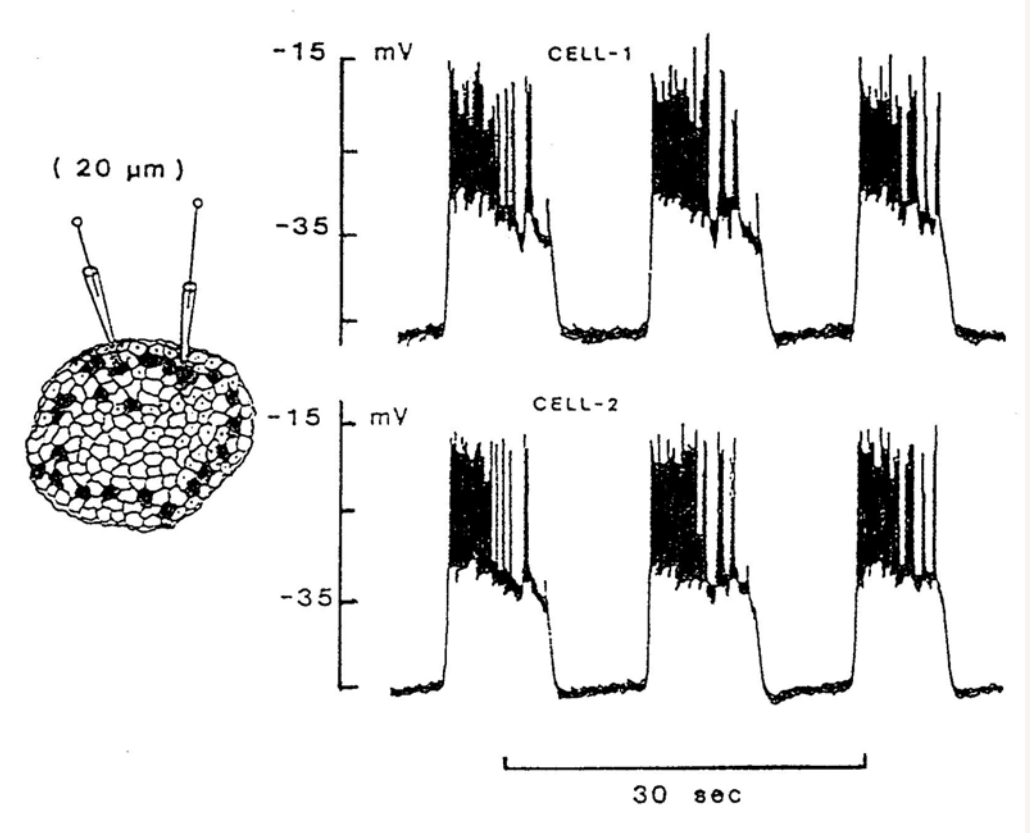

2:1 and 3:1Synchronization of Islet Insulin Secretion

The cells in a pancreatic islet (islet of Langerhans) interact to produce spontaneous oscillations in the overall insulin secretion with a period of about 5 min.

These oscillations are completely smoothed out in the liver and, hence, considered as a signal to this organ.

By forcing an islet with a periodic variation in the glucose concentration of the surrounding fluid, one can observe 1;2 or 1:3 synchronization in which the islet displays 2 or 3 pulses of insulin secretion per period of glucose oscillation.

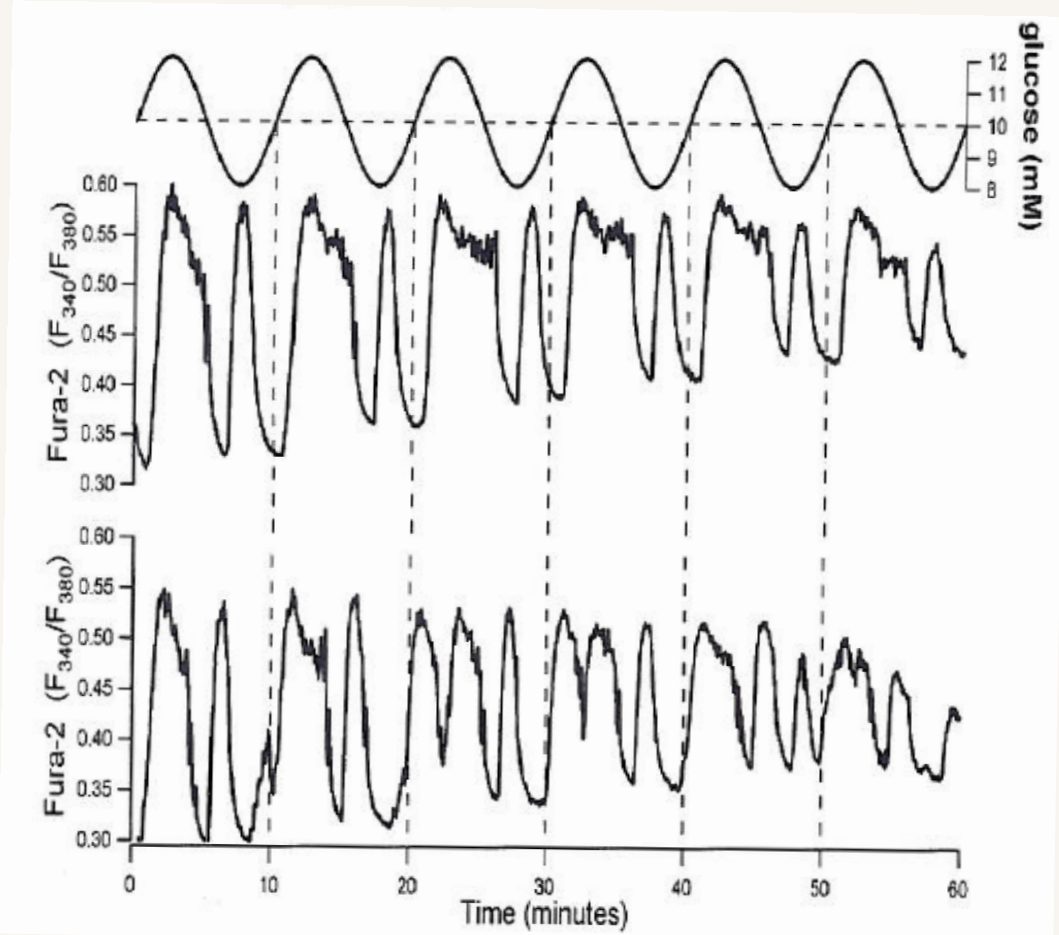

D. S . Luciani, 2004

Response of Noise Inflicted Cold Receptor

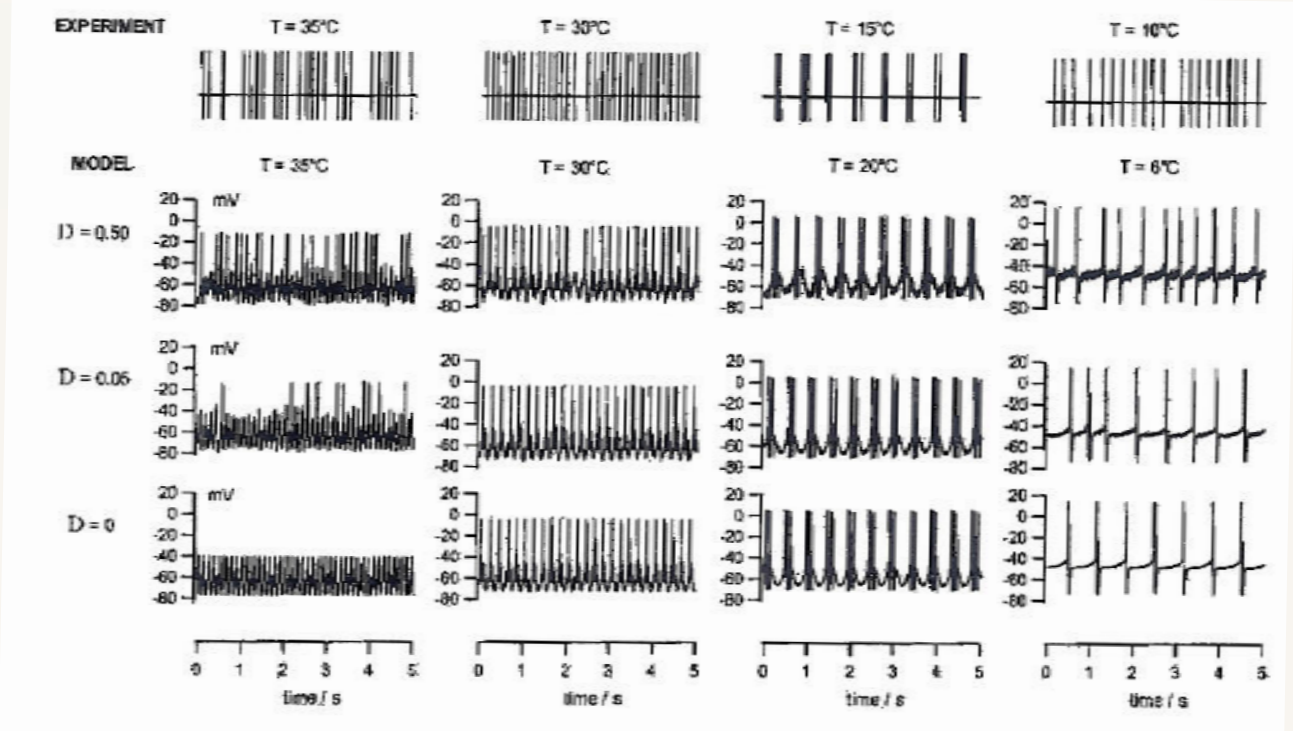

With Hans Braun, Marburg

D is a measure of the noise intensity in the simulations.

The spiking frequency increases with temperature whereas the amplitude of the cellular oscillations that trigger the spikes decreases.

At low temperatures the presence of noise leads to random shifts in the spiking time. At normal skin temperature, noise causes spike skipping. At high temperatures, noise is required to elicit spiking from the sub-threshold oscillations (stochastic resonance).

Interference Microscopy: The Phase Height Relief

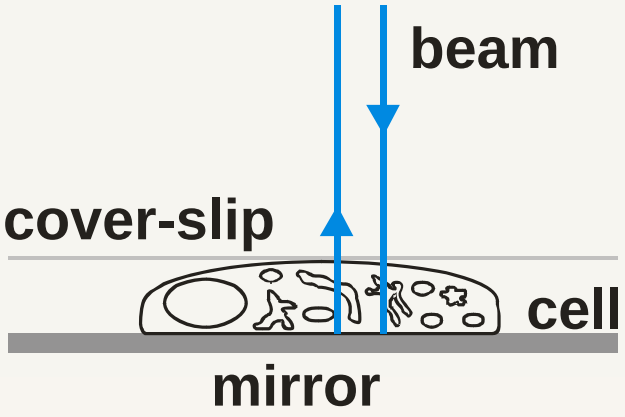

The delay of the light beam depends on the cell thickness, the presence of various organelles in the cytoplasm, the plasma membrane structure, etc.

For erythrocytes we can detect changes in the distribution of hemoglobin and in the micro-tubular structure below the cellular membrane.

Raman scattering studies allow us to determine changes in the hemoglobin binding capacity and the ability to release oxygen.

The cellular phase height relief can be obtained from:

$$\Phi = \frac{(\varphi_0 - \varphi_{obj})}{2\pi}\frac{\lambda}{2} - \Phi_0$$

With Nadia and Alexey Brazhe
Dept. of Biophysics, Moscow University

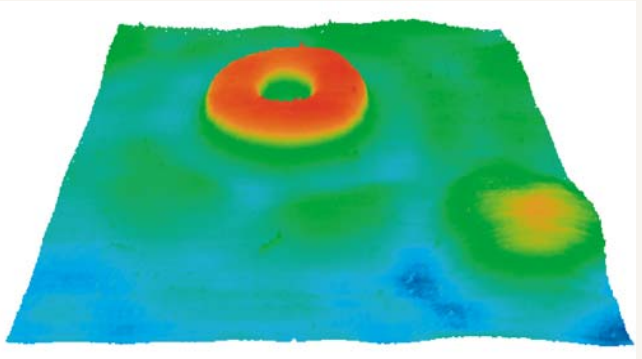

Isolated Neuron of the Pond Snail L. Stagnalis

Optical photograph (a) and a phase height relief (c) of a neuron. (b) magnification of tip structure. (c) displays the phase height along the scan-line shown in (b).

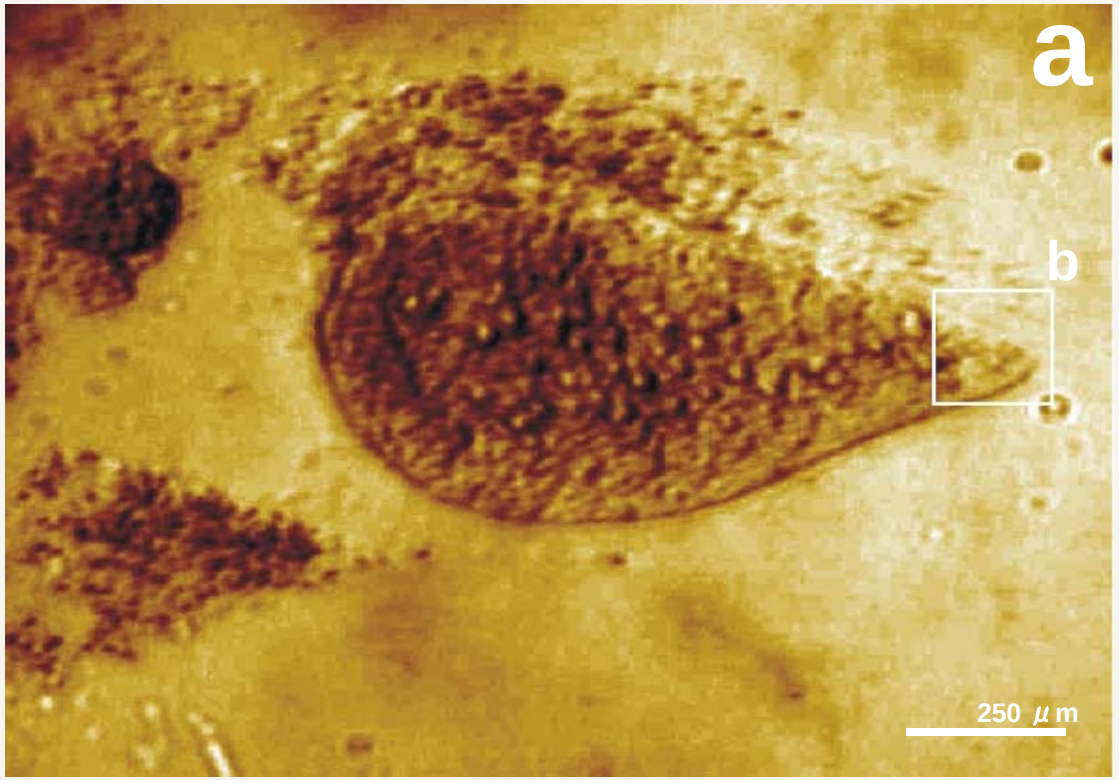

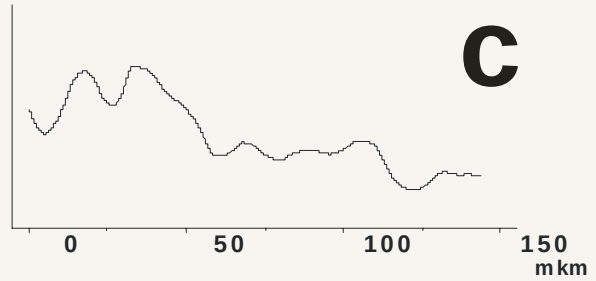

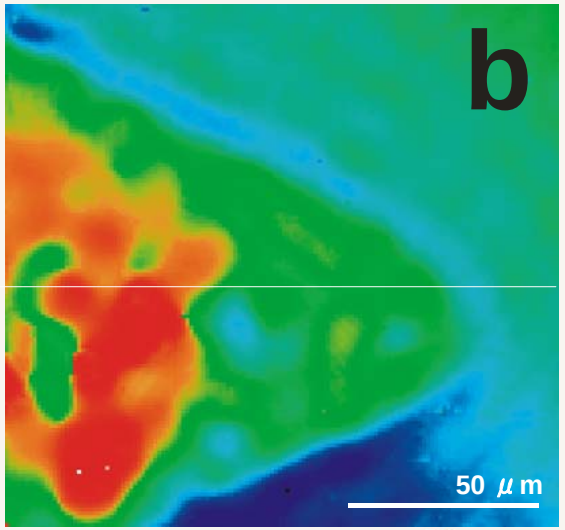

Time-Resolved Interference Microscopy

Among the cellular processes that manifest themselves through changes in the phase height relief are:

- Shape and volume changes
- Rearrangements of organelles and vesicle motion
- Electrical activity and motion of membrane bound proteins
- Changes in membrane fluidity and motion of microvilli
- Sorption and desorption of membrane bound Ca^{2+} ions

Double-wavelet techniques allows us to detect local temporal variations of the various oscillatory components and determine their mutual modulation effects.

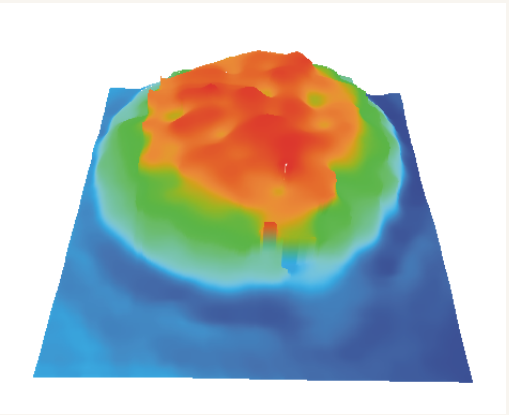

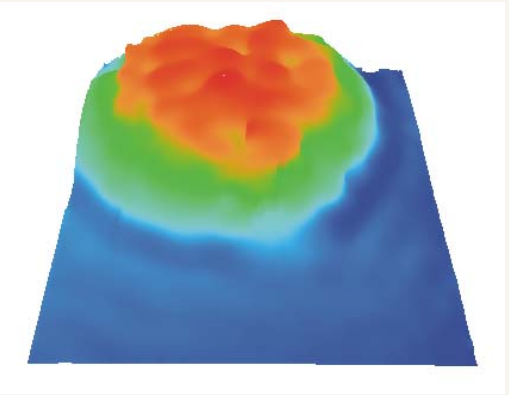

Frequency Modulation of High Frequency Modes

Double-wavelet analysis of the results obtained for neurons of *L.stagnalis*.

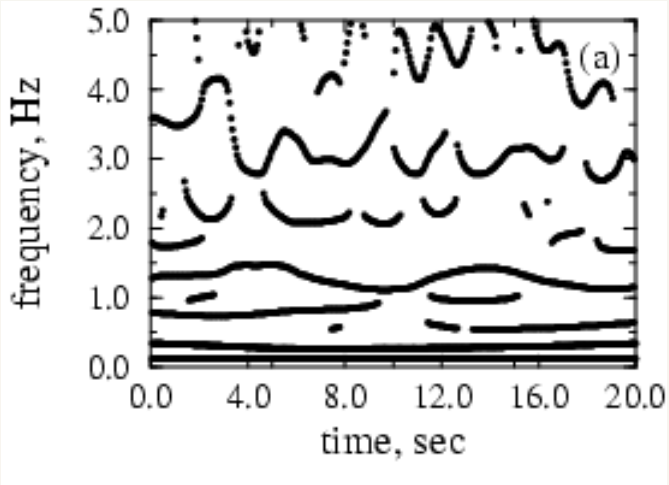

Typical dynamics of the local maxima of the energy density for the low frequency range (a). The observed 0.1, 0.3, 0.8, 1.3, and 2-4 Hz rhythms represent different components of the cellular dynamics.

Note how the 1.3 Hz component is modulated by a signal with a 10-sec period, i.e. by the 0.1 Hz signal.

Chemical Reaction Cascades

1. Single reaction step

$$\frac{dS}{dt} = \frac{aS_o}{b + S_0} - \frac{S}{\tau}$$

Equilibrium: $S_{eq} = \frac{a\,\tau S_o}{b + S_0}$

Eigenvalue: $\lambda = -\frac{1}{\tau}$

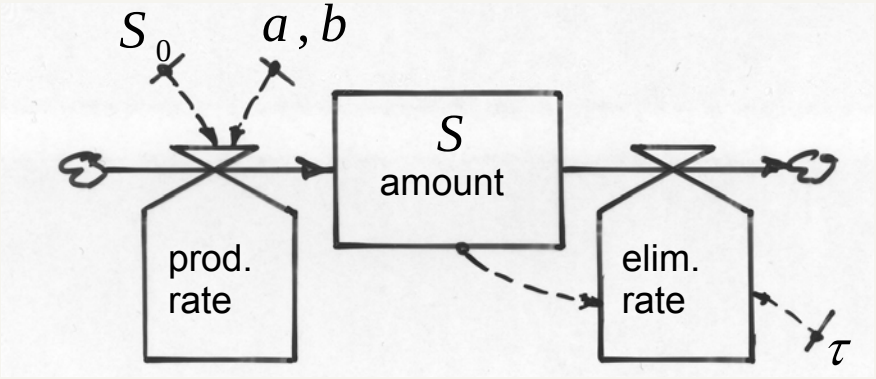

2. Reaction cascade

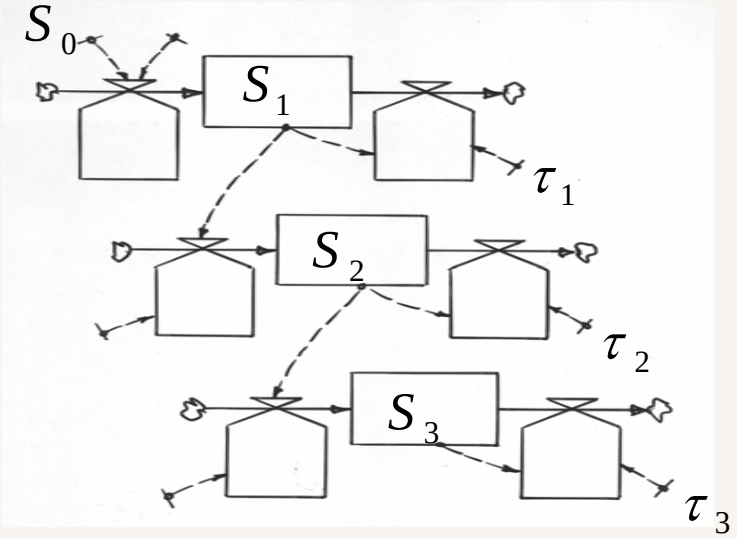

$$\frac{dS_1}{dt} = \frac{a_0 S_o}{b_0 + S_0} - \frac{S_1}{\tau_1}$$

$$\frac{dS_2}{dt} = \frac{a_1 S_1}{b_1 + S_1} - \frac{S_2}{\tau_2}$$

$$\frac{dS_3}{dt} = \frac{a_2 S_2}{b_2 + S_2} - \frac{S_3}{\tau_3}$$

Eigenvalues: real and negative

Close the Loop – And Watch Oscillations Arise

3. Negative feedback

Eigenvalues can become complex conjugated: Oscillatory response can arise

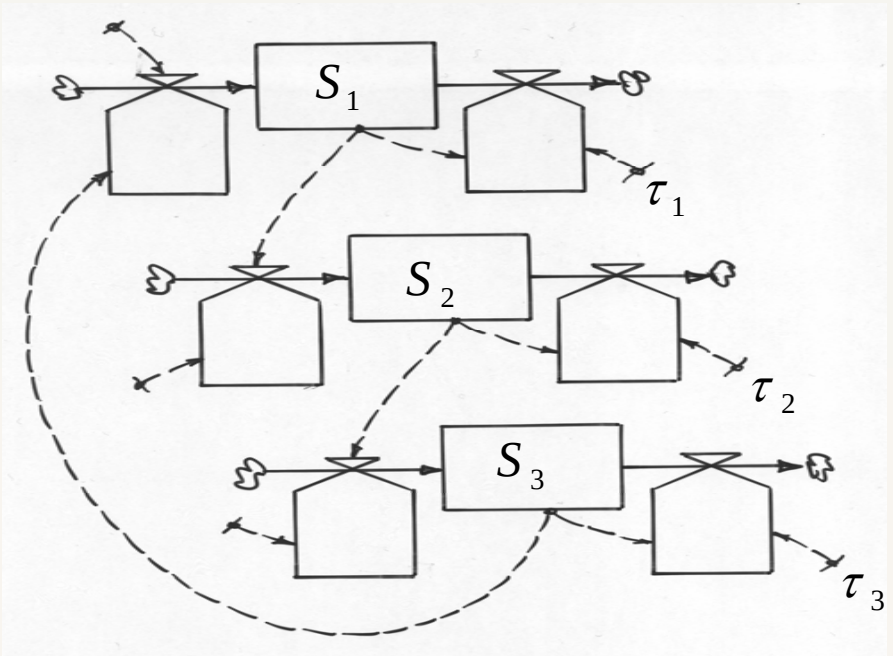

4. Larger loop gain

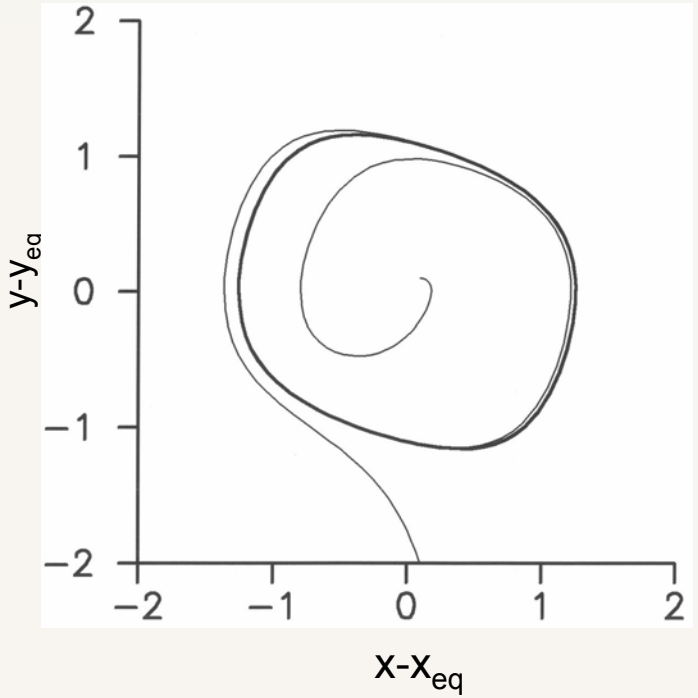

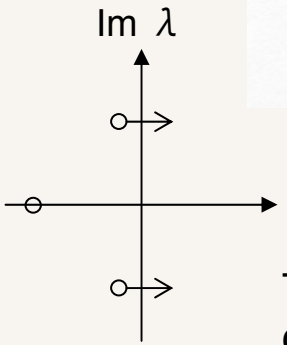

Two complex conjugated eigenvalues may cross the imaginary axis. The equilibrium point turns unstable (Hopf bifurcation) and the system starts to perform self-sustained oscillations.

It Doesn't Move – It's Probably Dead

- Oscillatory phenomena typically arise from negative feedback mechanisms with delays.
- Oscillations may serve as pacemakers or biological clocks that can coordinate different processes in time.
- Interaction between two or more oscillatory processes produces complex temporal phenomena and various forms of synchronization.
- The cells, functional units, etc. actively make use of the complex temporal patterns intheir mutual communication.

Changes in the temporal patterns can be part of a normal physiological regulation, or signal a state of disease

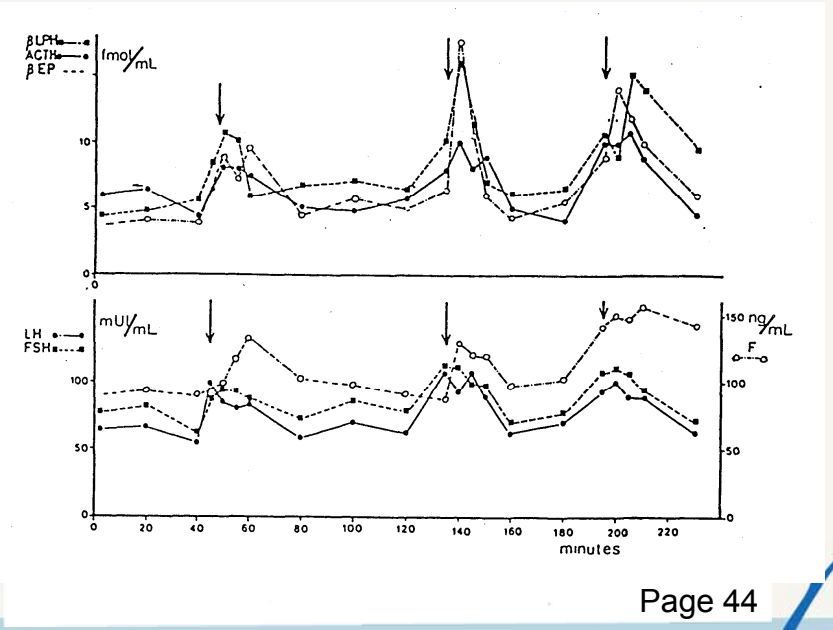

Simulating the Response to a Series of Meals

The timing of the meals and their volumes in terms of equivalent glucose contents are specified exogenously.

For the healthy person, the increase in blood glucose is accompanied by a rapid increase plasma insulin concentration.

By virtue of the nonlinear character of the model, the response to a given meal depends of its timing and size relative to previous meals.

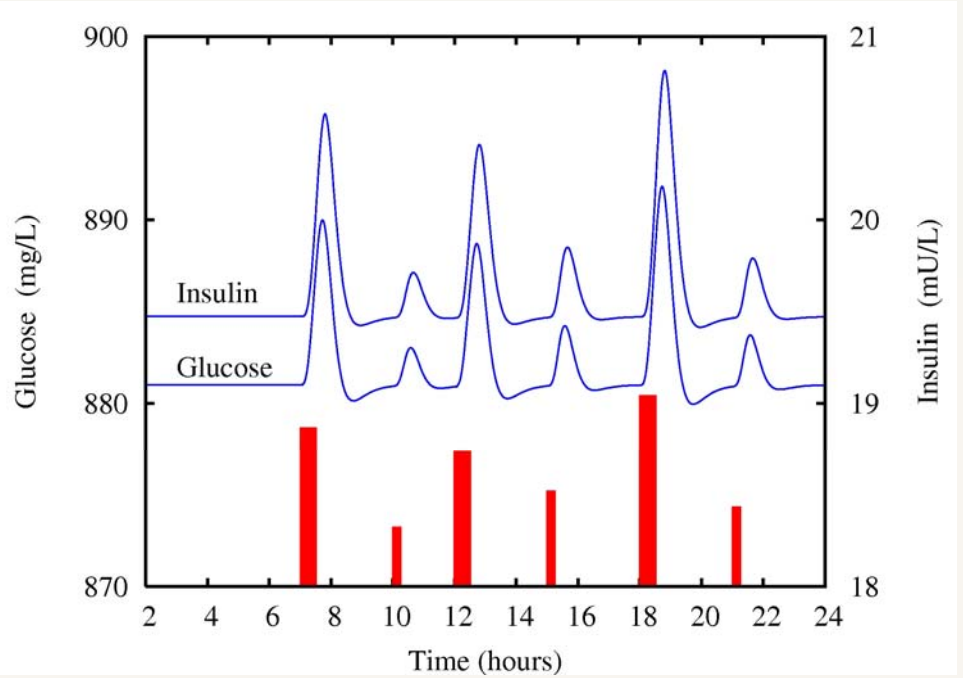

With appropriate extensions,accounting e.g. for the role of other metabolic substances (fat, protein, keton bodies, etc.), the model may be used to simulate more advanced issues of the metabolic control system.

Ultradian Pulses of Insulin Secretion

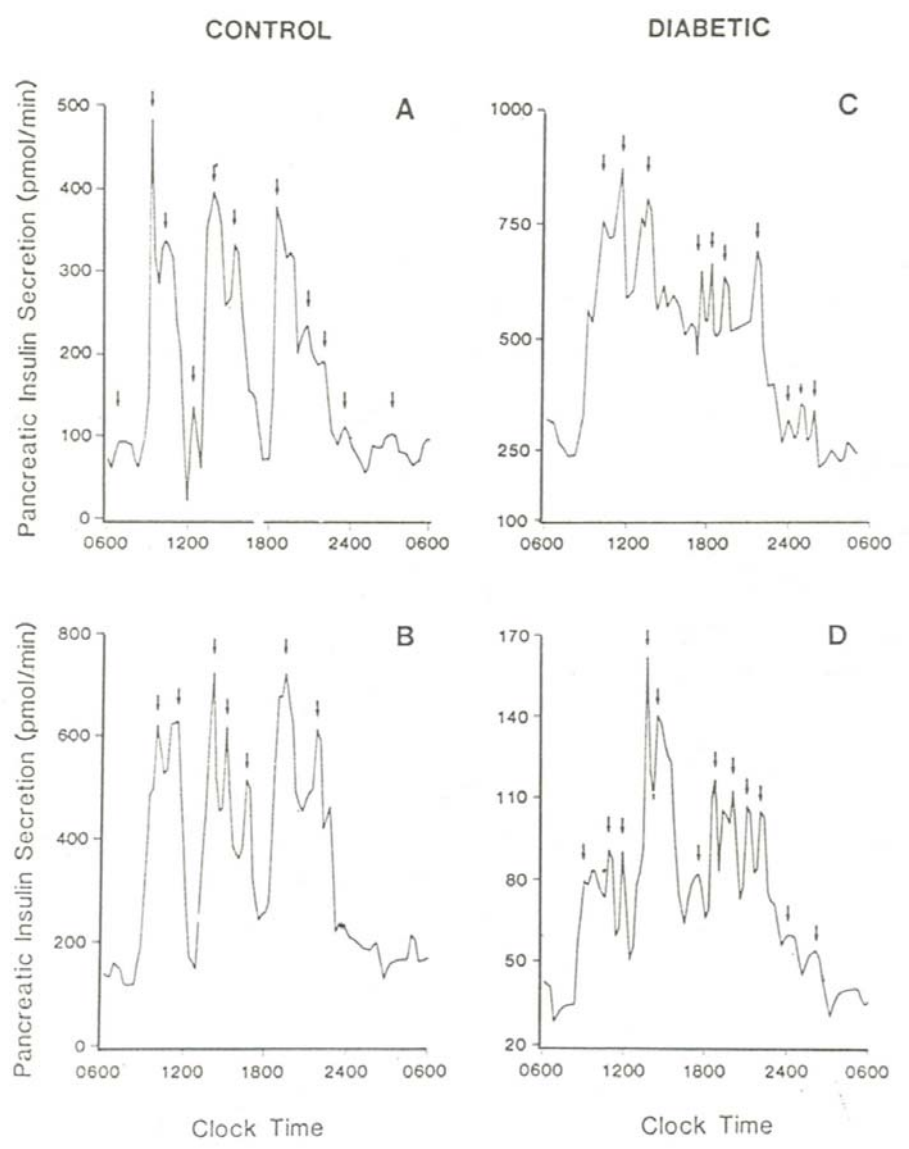

Polonsky et al. New Eng. J. Med. (1988).

24 h insulin secretion profiles for two type-II diabetics and two age-matched controls. 10 min. temporal resolution. Meals were eaten at 09.00, 13.00 and 18.00.

Arrows indicate statistically significant pulses of insulin secretion.

There is an obvious “ringing” in response to a meal. This is even more pronounced for type-II diabetics.

Can the “ringing” be used as a preclinical diagnostics of type-II diabetes?

Alternative Hypotheses for Pulsatile Insulin Secretion

- The ringing phenomenon is characteristic for an early stage of type-II diabetes and may be used for preclinical diagnosis?
- The ”ringing” represents a pulsatile release of insulin similar to the ultradian rhythms are known for many other hormones?
- The pulsatile release of insulin is triggered by signals from the brain, or caused by a pancreatic pacemaker?
- The oscillations are produced by a delay in the insulin-glucose feedback regulation. This delay is associated with the response of muscle and adipose tissue cells, or pancreatic β-cells?
- The oscillations are caused by processes in the liver (hepatic glucose release, glucagon)?
- The oscillations promote glucose uptake in the cells through interaction with the insulin receptor internalization dynamics?

Pulsatile Insulin Secretion in Fasting Subjects

Young healthy subject fasting during (and for 12 hours before) the experiments

Continuous intravenous glucose infusion at the rate of 6 mg/(kg min)

Blood samples were taken every 10 min and examined for glucose, insulin and C-peptide

Glucose-clamp experiments demonstrated that the oscillations were not associated with a pancreatic pacemaker

Experiments with patients having undergone pancreas transplantation showed that they were not caused by signals from the central nervous system.

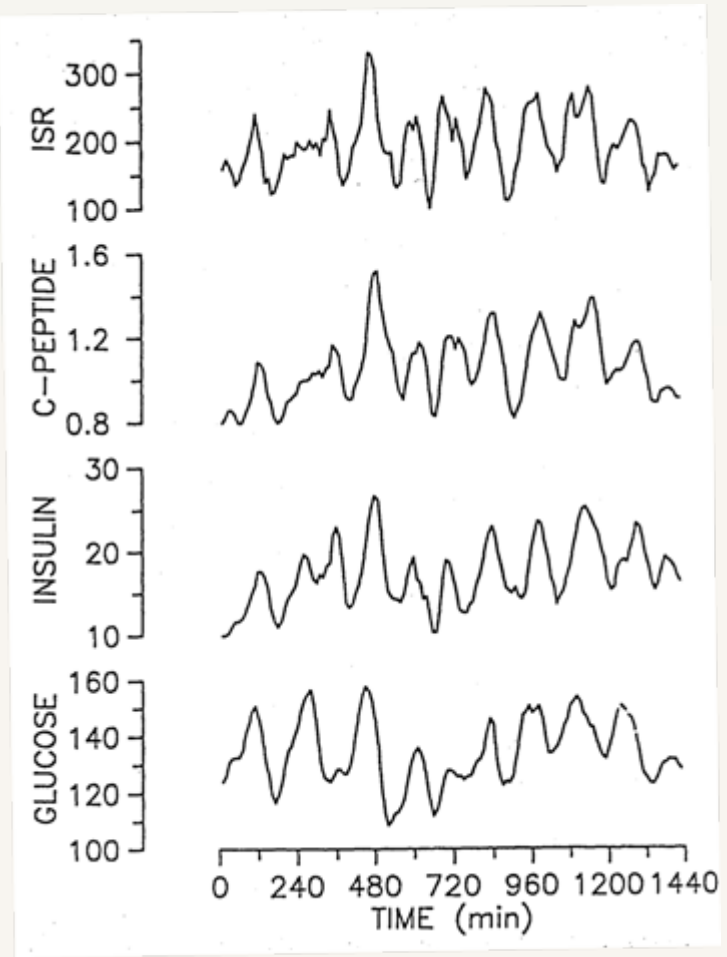

Sturis et al., Am. J. Physiol. (1991)

Extended Metabolism Model

Sturis et al., Am. J. Physiol. (1991)

The model accounts for:

- the finite equilibration rate of insulin between the plasma and interstitial volumes.
- the separate degradation of insulin in the two compartments
- the release of glucose from the liver at low insulin concentrations.
- parameters and nonlinear relations are determined through separate experiments.

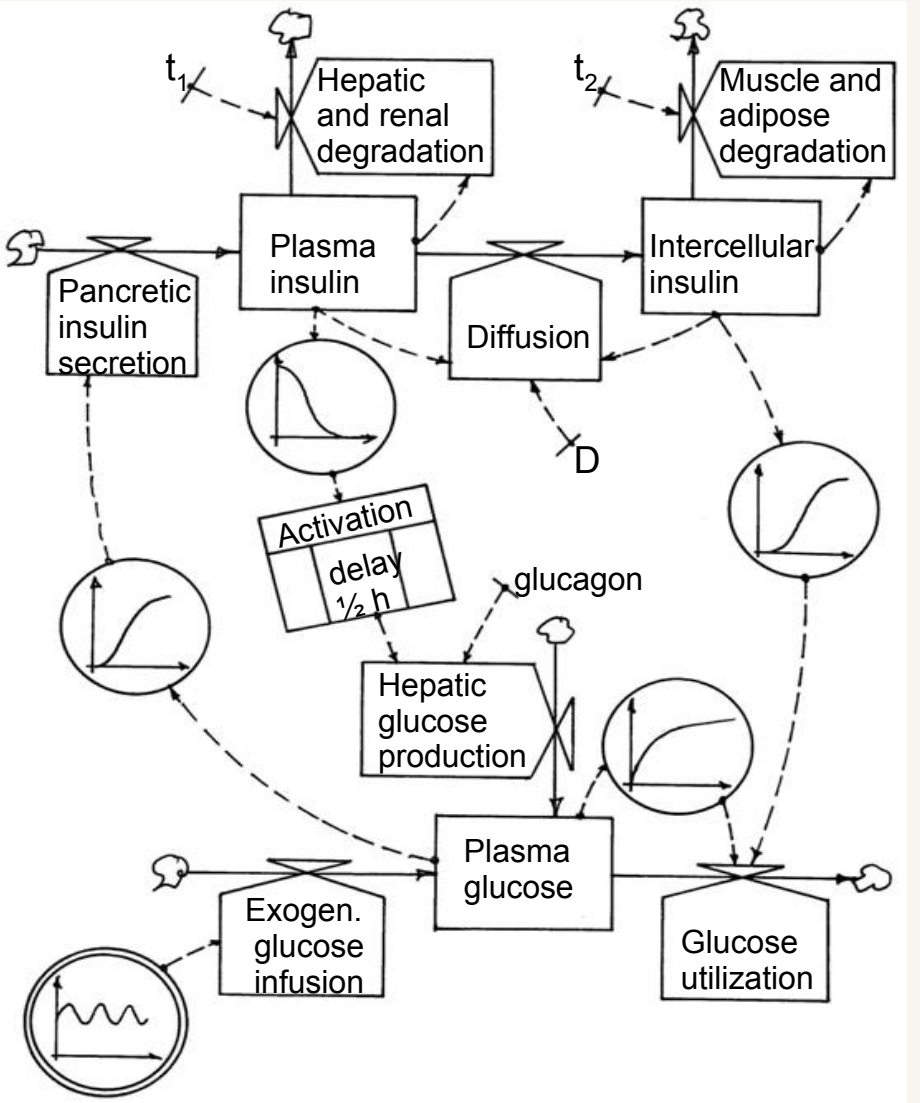

Self-Sustained Oscillations in Insulin Secretion

The model produces self-sustained oscillations with a period of about two hours.

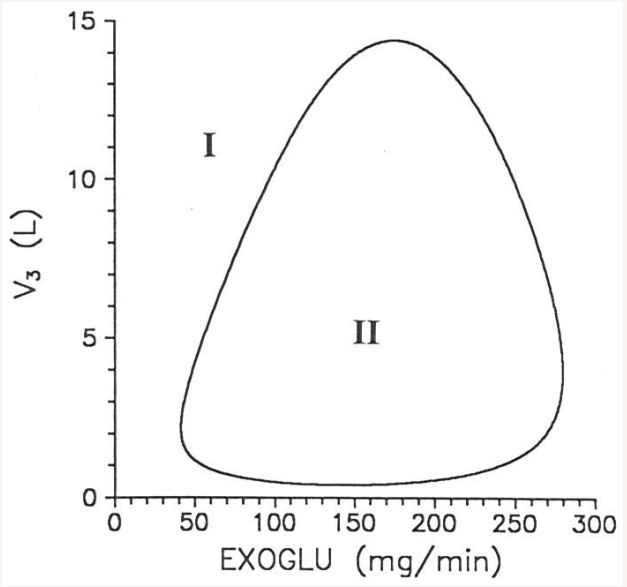

Oscillations only occur in a limited region of parameter space around the normal operational regime. The model is stable both for very small and very large blood glucose concentrations.

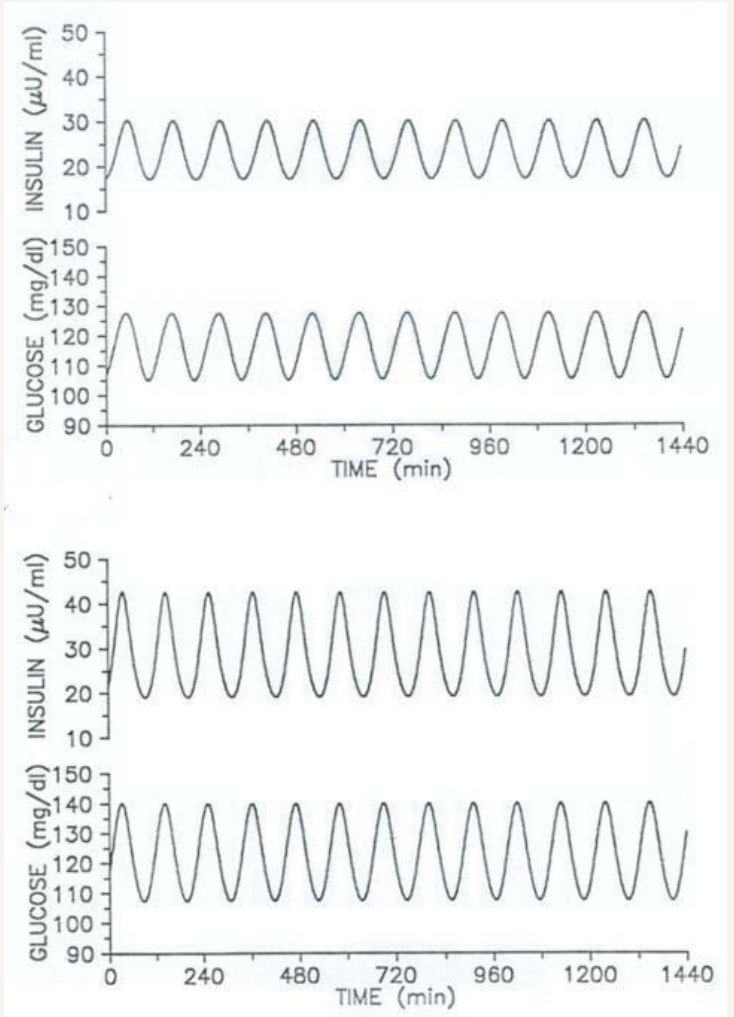

External Forcing of the Insulin Secretion

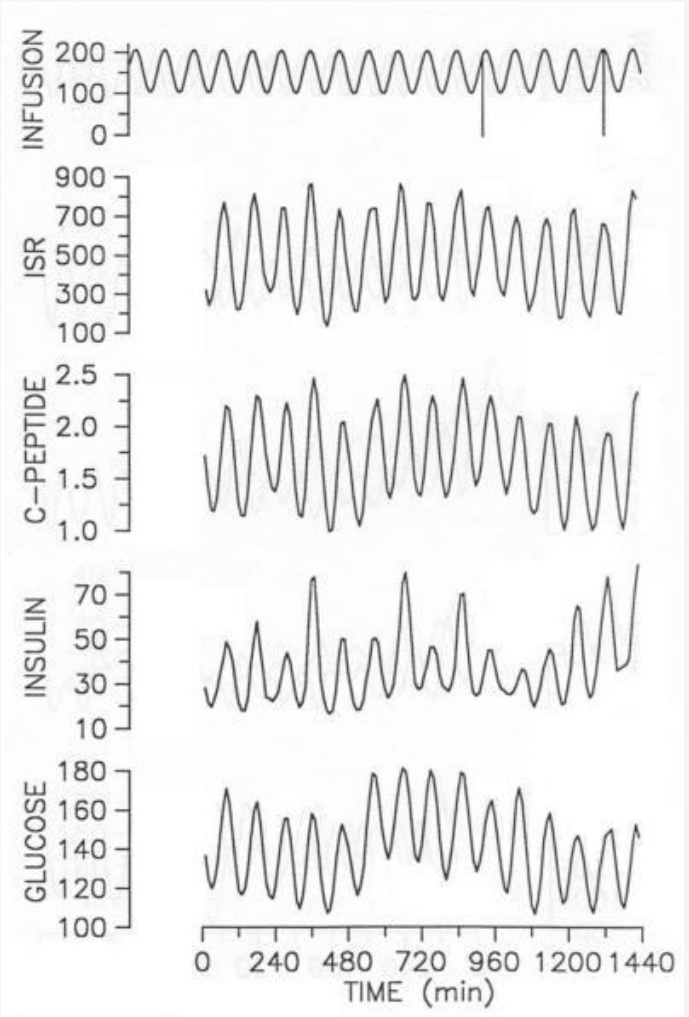

- The secretion of insulin can synchronize with the periodically varying glucose infusion.
- By studying the ability to synchronize as a function of the amplitude and frequency of the oscillatory glucose infusion, one can determine the strength of the nonlinear interactions in the system.
- If the same period is observed in other variables, one can conclude that they are coupled to the insulin secretion.

2:1 Synchronization of the Insulin Secretion

Sturis et al., Chaos (1995)

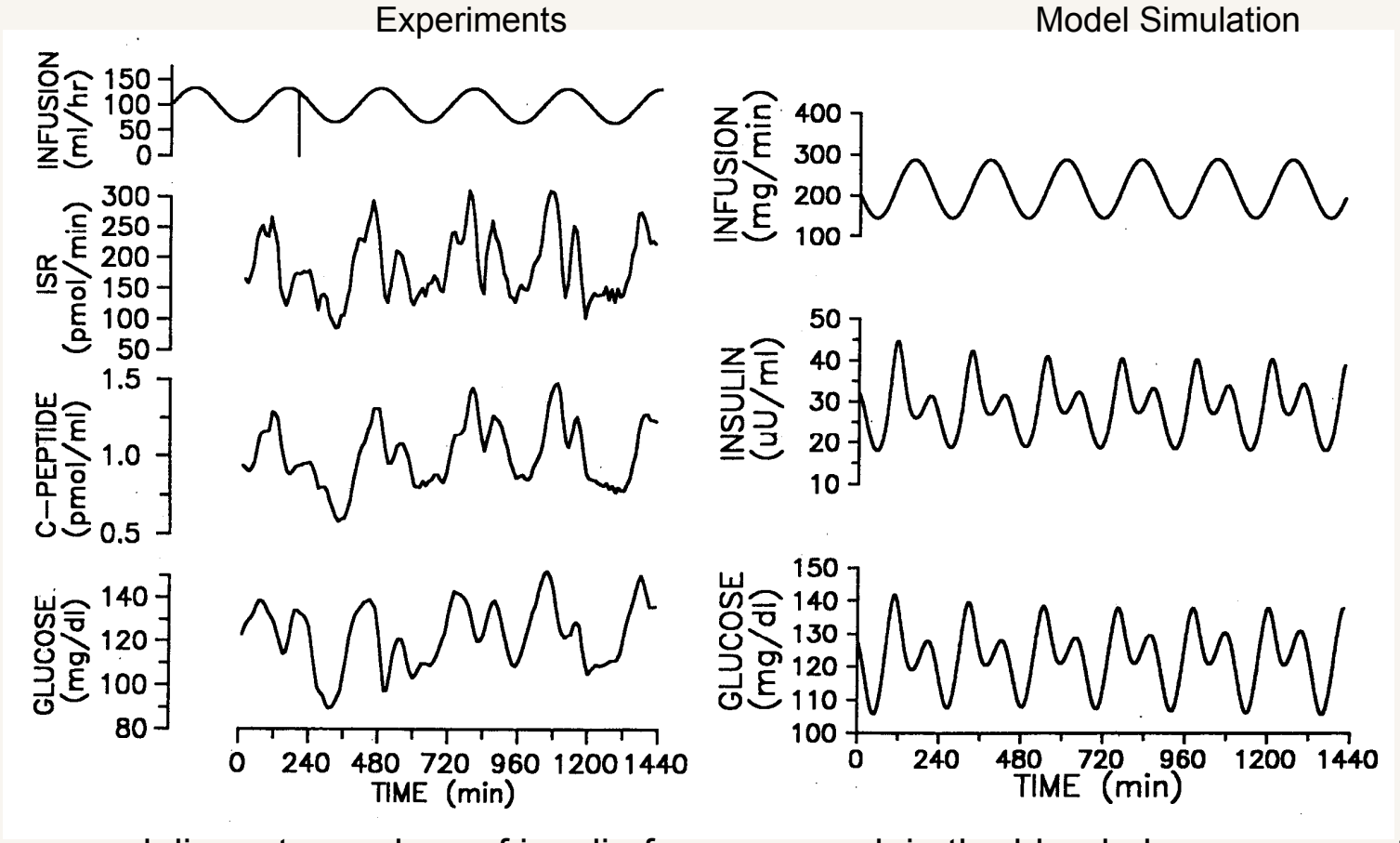

The pancreas now delivers two pulses of insulin for every peak in the blood glucose concentration.

Bursting and Spiking Pancreatic Beta-cells

- Isolated beta-cells tend to produce randomly looking spike sequences in their membrane potentials.
- Intact cells in pancreatic islets produce bursts of spikes with a bursting fraction that varies with the glucose concentration
- Insulin is released during the bursting period. Isolated cells typically release insulin at significantly lower rates than islet cells.
- The bursting dynamics arises from the interaction between a fast potassium dynamics and a slower calcium dynamics. The electrophysiological processes again couple to metabolic oscillations in the cell.

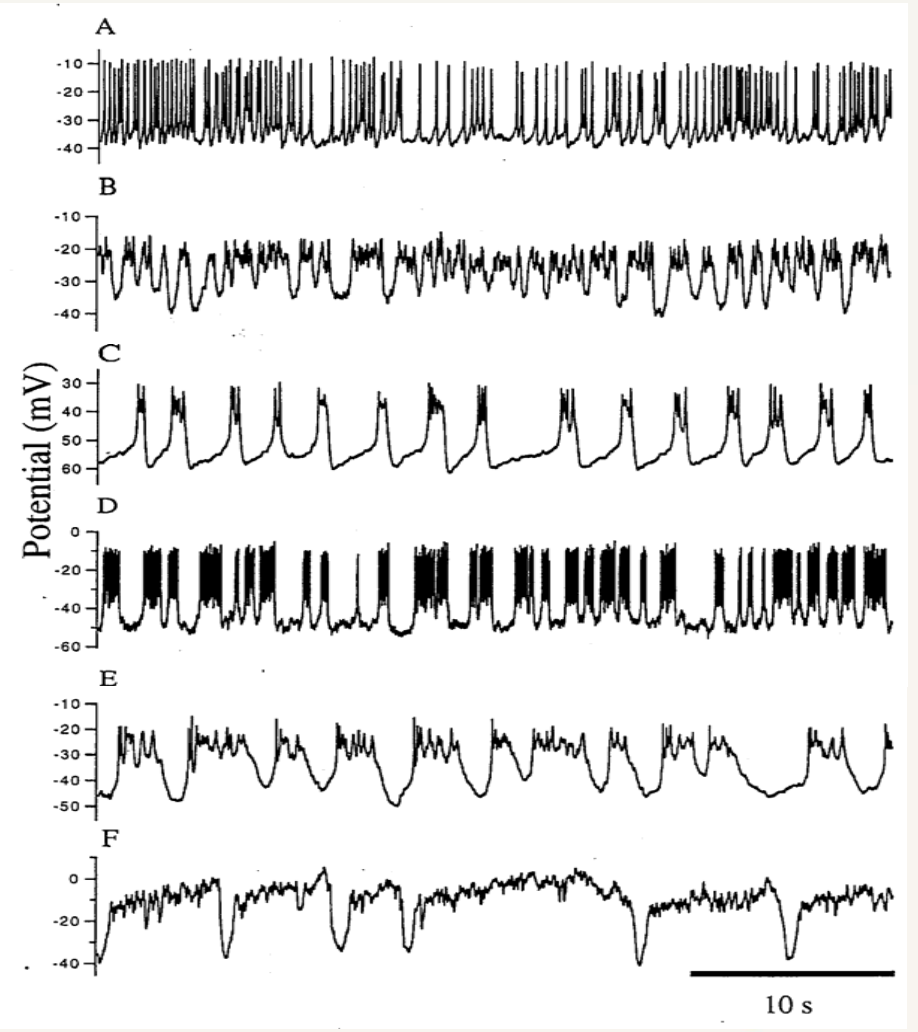

The Sherman β-Cell Model

Models of pancreatic beta-cells are usually based on standard Hodgkin-Huxley formalism with possible elaborations to account for intracellular calcium storage, various aspects of the glucose metabolism, intracellular insulin transport, etc.

At a minimum, a 3-dimensional model with two fast variables and one slow variable is required to generate a robust bursting behavior.

In the Sherman model, the fast variables are the membrane potential *V* and the opening probability of the potassium channels *n*. The slow variable *S* is related to the intracellular calcium concentration.

$$\tau \frac{dV}{dt} = -I_{Ca}(V) - I_K(V,n) - g_s S(V - V_K)$$

$$\tau \frac{dn}{dt} = \sigma(n_\infty(V) - n)$$

$$\tau_S \frac{dS}{dt} = S_\infty - S$$

with

$$I_{Ca}(V) = g_{Ca} m_\infty(V)(V - V_{Ca})$$

$$I_K(V,n) = g_K n(V - V_K)$$

$$z_\infty = \left[1 + \exp((V_z - V)/\theta_z\right]$$

$$z = m,\ n \text{ and } S$$

Simulating a Bursting β-Cell

- Temporal variation shows the gradual rise of the slow variable during the bursting phase.
- At a certain point the bursting stops, the slow variable starts to decline, and the membrane potential attains its resting value.
- As the slow variable becomes sufficiently small, a new bursting period is initiated.

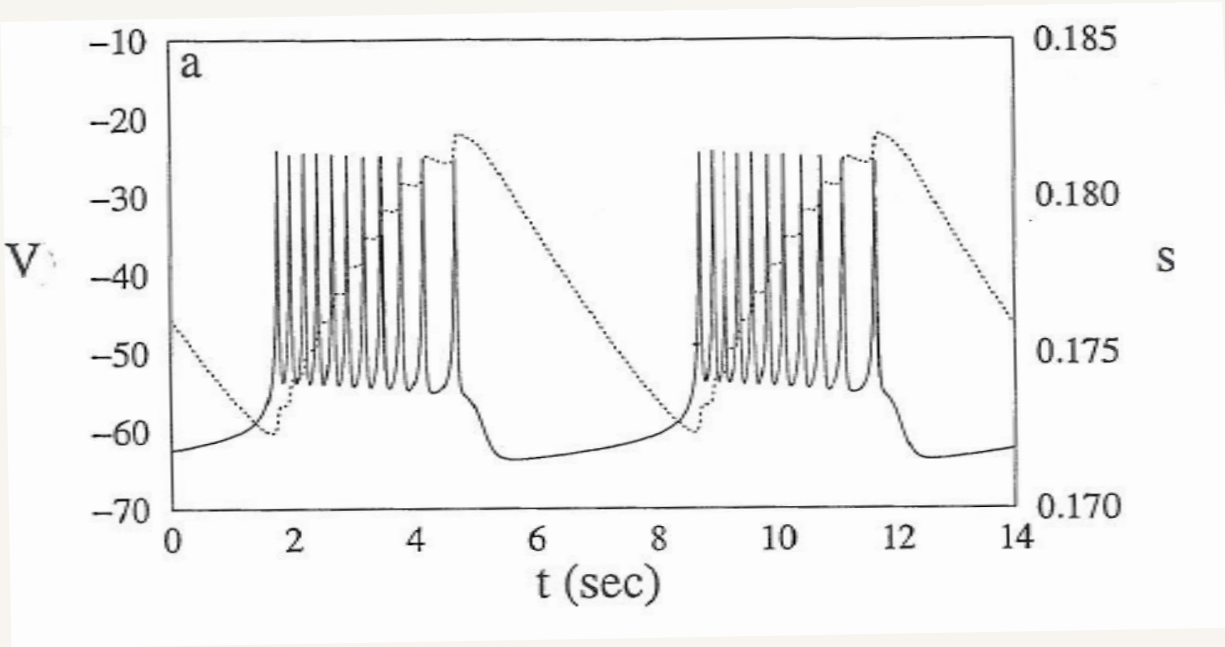

The bursting periods are controlled by the time scales, the conductances, and the opening probabilities of the various ion channels, particularly by the rate at which calcium is pumped out of the cell.

The Bursting Mechanism

- Considering the enormous ratio between the two time scales (appr. 500), the discussion typically proceeds by treating the slow variable as a bifurcation parameter for the fast subsystem.
- In the *SV*-plane, the equilibrium point for the fast subsystem exhibits two saddle-node bifurcations and a Hopf bifurcation.
- The slow isocline intersects the unstable branch of the equilibrium point curve. To the left of this isocline S increases with time and to the right S decreases.
- Moreover, a homoclinic bifurcation takes place in the collision of the limit cycle oscillator with the unstable branch of the equilibrium point curve.

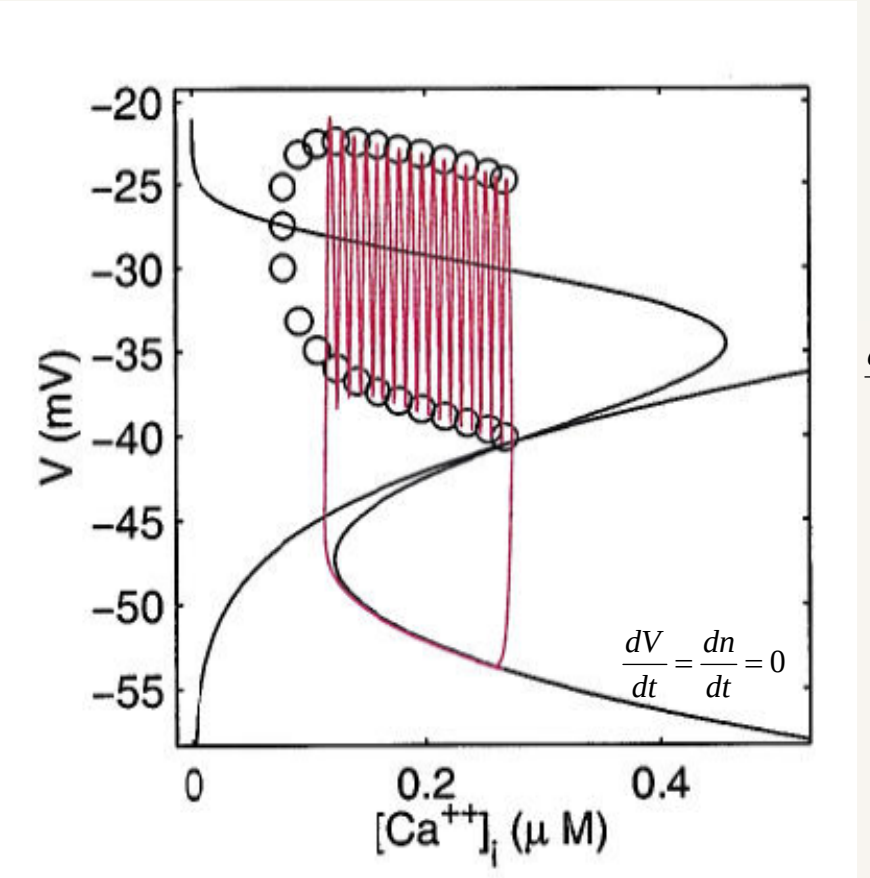

Bifurcation Diagram for Bursting β-Cell

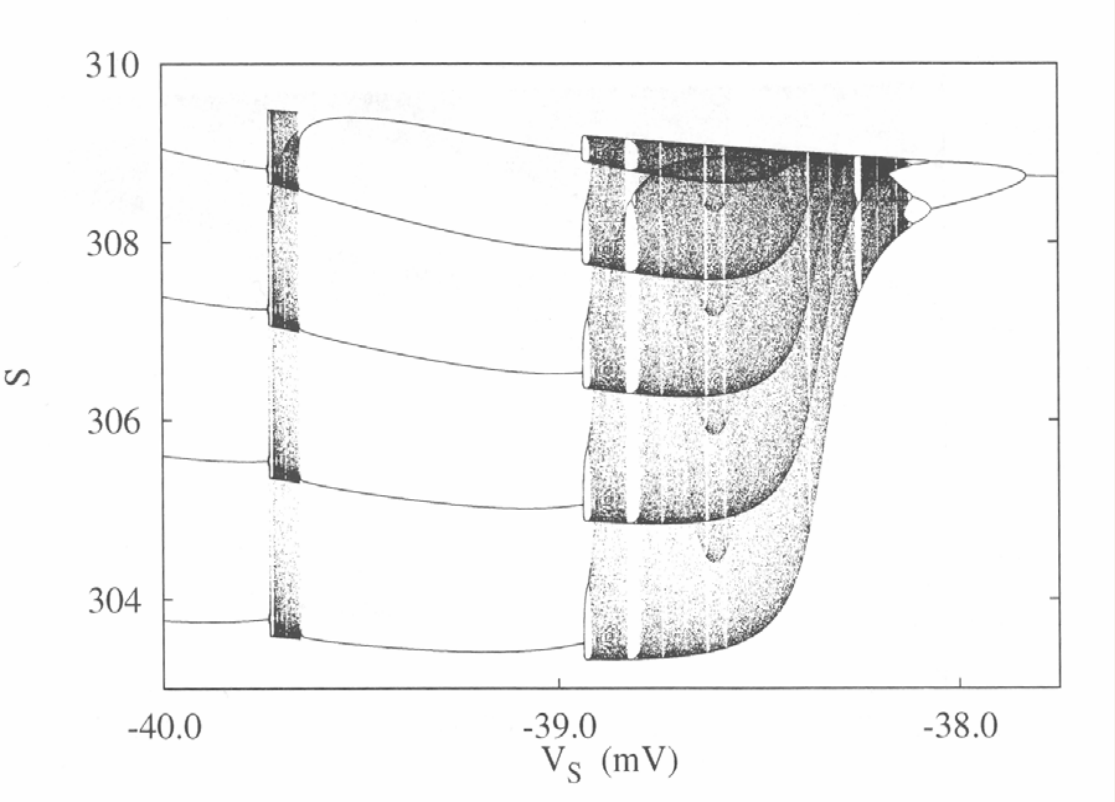

- To the right in the diagram (V_s=-37.8 mV) the model displays tonic firing.
- As V_s is reduced the model develops through a period-doubling cascade to deterministic chaos.
- To the left in the figure the model displays regular bursting with four spikes per burst.

- Transition from four to five spikes per burst takes the model through another region with deterministic chaos.

2D Bifurcation Structure

Vertical: Ratio between time scales
Horizontal: Nernst potential for slow variable

A vertical scan to the right in the diagram appears to show a normal period-doubling bifurcation cascade leading to chaos and various periodic windows.

Further to the left in the diagram, the bifurcation curves start to intersect, and the system displays a so-called 'period-adding' sequence.

This is accompanied by the period-doublings becoming subcritical.

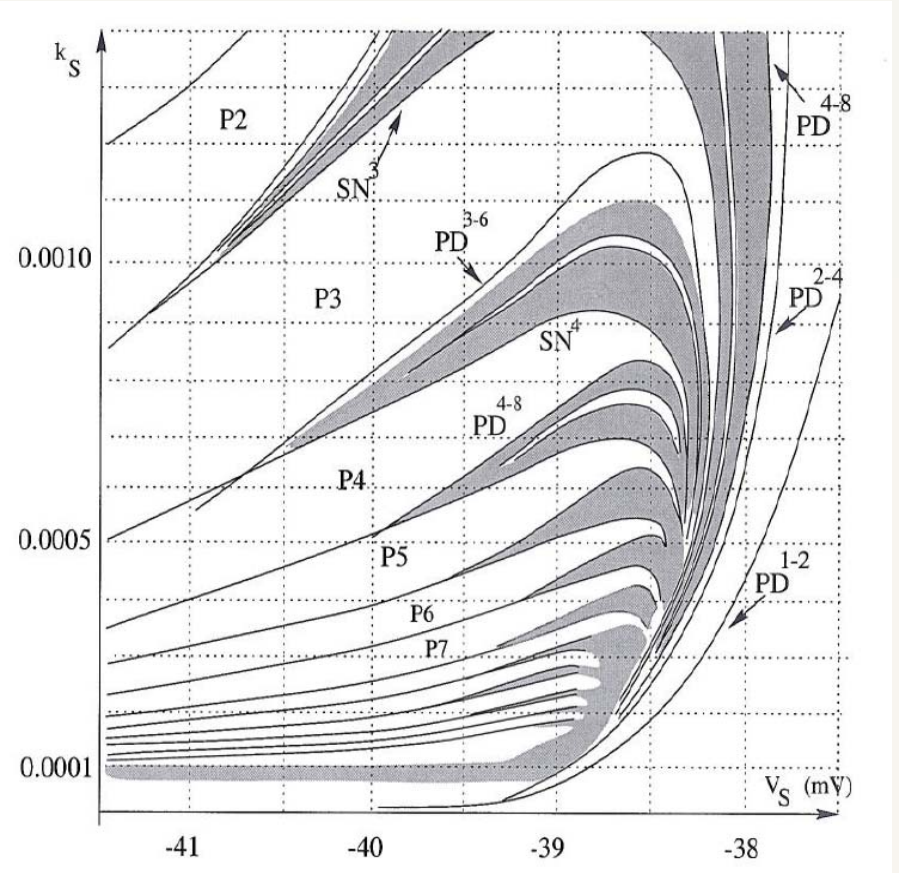

Folding of the Bifurcation Structure

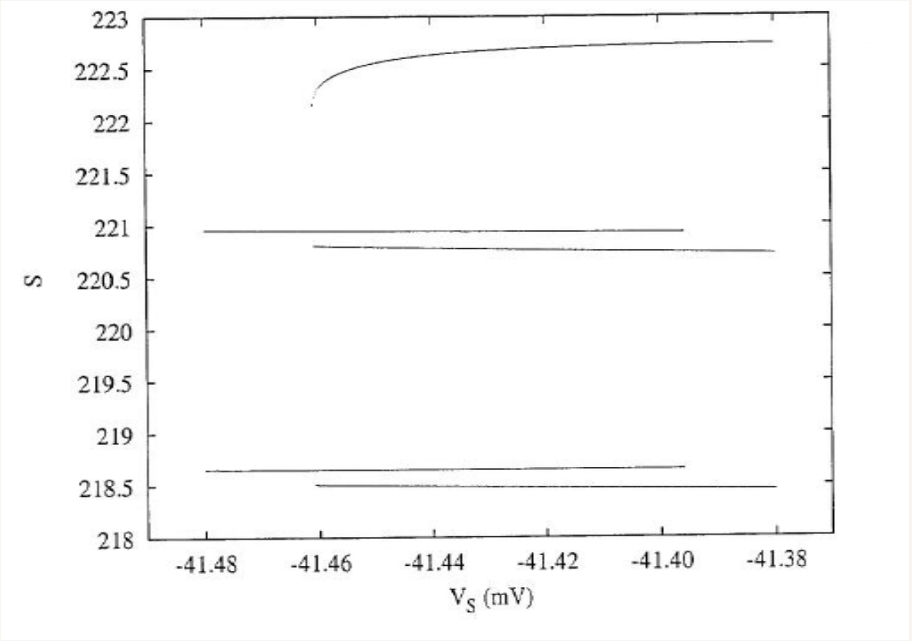

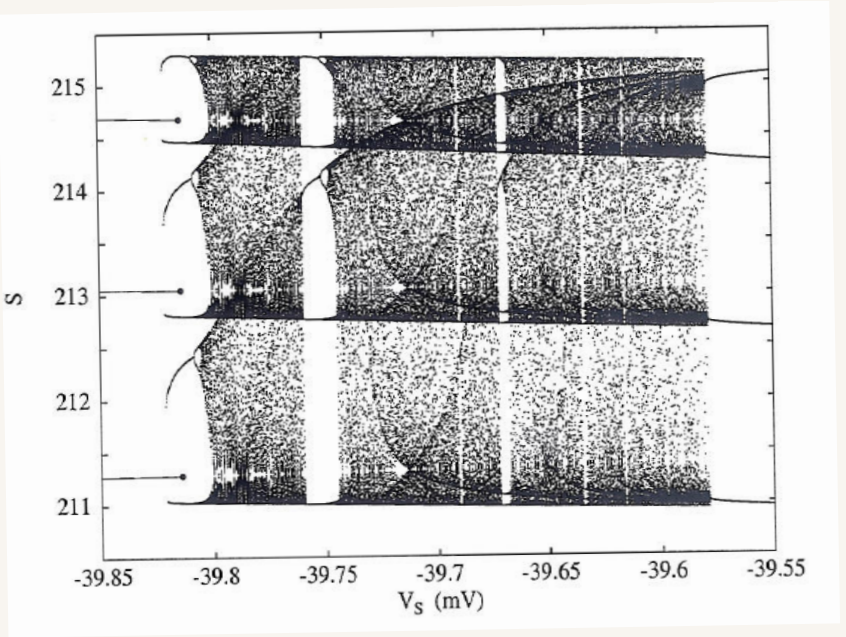

Left: The period-2 solution destabilizes in a subcritical period-doubling bifurcation well into the period-3 vindow. The period-3 solution arises as usual in a saddle-node bifurcation.

Right: The period-3 solution destabilizes in a subcritical period-doubling bifurcation. As the ratio between the time scales becomes larger, the subcriticality becomes even more pronounced, and part of the chaotic solutions disappear through collision with the unstable period-solution.

Deep Brain Stimulation of Parkinson's Disease

Peter Tass, Jülich Research Center

Purpose: To define a stimulation schedule that is less invasive than the schedule presently used: 0.1 ms pulses of 1.5-3.0 V and 130 Hz.

Model: A population of globally/locally coupled phase oscillators:

$$\dot{\Psi}_j = \omega_j - \frac{K}{N}\sum_{k=1}^{N} \rho^{c}_{jk} \sin(\Psi_j - \Psi_k) - K_m \sum_{i=1}^{4} \rho^{s}_{ji} \sin(\Psi_j - \Phi_{\tau_i}) + F_j(t),$$

Where ω_j represents the internal dynamics of the uncoupled oscillator, the 2nd term represents the coupling, the 3rd term the delayed feedback of the mean phase, and the 4th is random noise.

Results: By analysing this simple model it has been possible to show that desynchronization of the spiking cells can be achieved in demand controlled mode by using a delayed signal from the brain of a much lower amplitude.

Application of this method on patients shows that it can produce long-lasting beneficial effects.

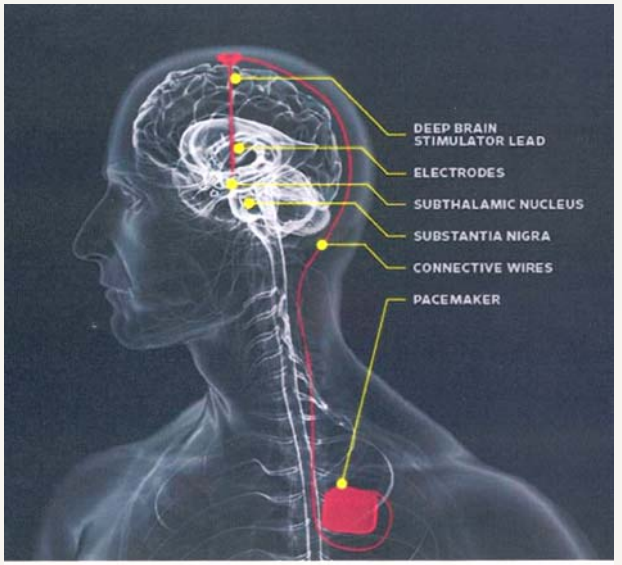

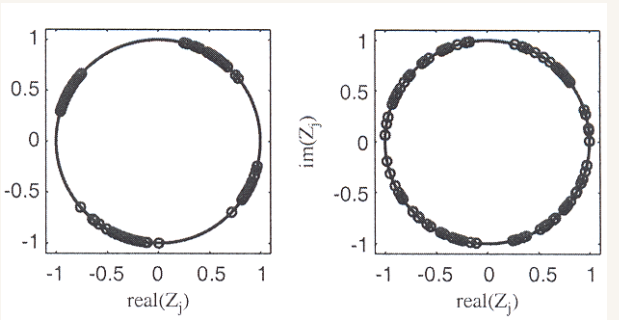

Interacting Substructures of the Brain

Anne Beuter, University of Bordeaux

Purpose: By means of a multi-scale population density approach to identify substructures of the motor loop that can be stimulated at lower risk and with higher efficiency than the subthalamic nucleus.

Cell model: $\frac{dv}{dt} = 0.04v^2 + 5v + 140 - u + I(t)$ $\frac{du}{dt} = a(bv - u)$ + reset mechanism

As *a* and *b* are varied, the Izhikevich model reproduces the main spiking and bursting behaviors characteristic of nerve cells.

Population density approach:

$$\frac{\partial}{\partial t} p(\vec{w}, t) = -\vec{\nabla}\left(\begin{bmatrix} 0.04v^2 + 5v + 140 - u + I(t) \\ a(bv - u) \end{bmatrix} p(\vec{w}, t) + \hat{e}_v \sigma(t) \int_{v-\epsilon}^{v} p(\tilde{v}, u, t) d\tilde{v}\right)$$

Results: Preliminary evaluation of the different substructures of the motor loop. Demonstration of the appearance of sustained oscillations through delayed signal transmission between the substructures.

Advantages: Computer time is independent of the number of neurons. Model can be extended with more physiological cell models, different cell types, and different types of interaction.

Simulation of Coupled Smooth Muscle Cells

Jens Christian Brings Jacobsen, University of Copenhagen

Purpose: To examine the mechanisms underlying the gradual recruitment of smooth muscle cells into the synchronized state, the present of quiescent cells, and the change of the oscillation frequency with increasing stress.

Model: The model considers a cluster of 17 cells and combines an electrophysiological model with a model of intercellular calcium dynamics (calcium-induced-calcium release, CICR from the Sarcoplasmic Reticulum).

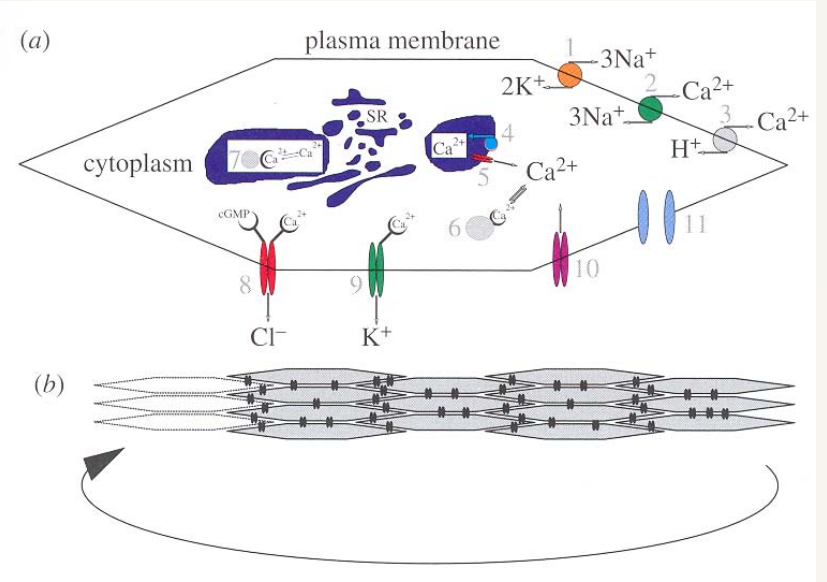

Neighboring cells are coupled electrically through gap junctions. Membrane depolarization causes opening of voltage-sensitive calcium channels and influx of calcium, leading to activation of CICR. Hereby, the local calcium wave is transformed into global oscillations in calcium concentration and muscular contraction.

Results: The model explains the gradual transition from random intracellular calcium waves to synchronized muscular contractions in terms of cellular inhomogeneity.

Virtual Physiological Human: The Heart Model

Dennis Noble, Oxford University

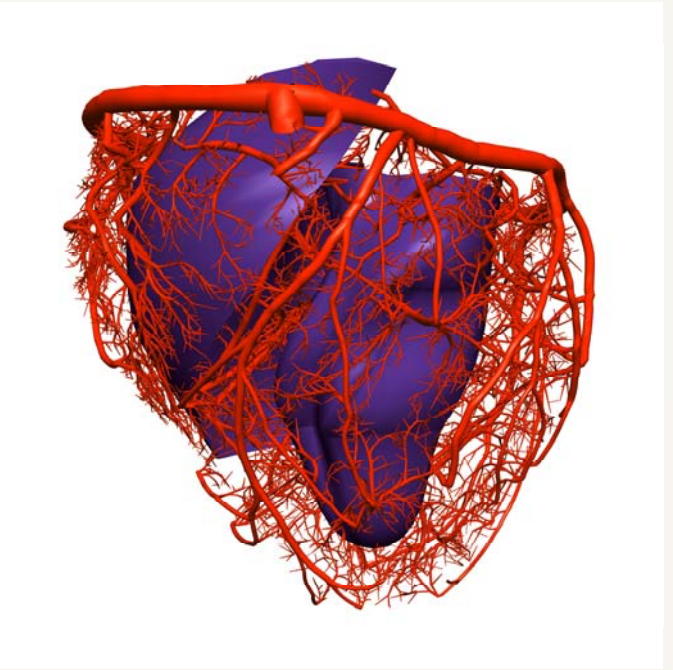

Purpose: To demonstrate the possibility of integrating cellular dynamics into a full scale model of the heart.

Model: The model provides a cell-accurate 3D reconstruction of the human heart. It describes the propagation of contractive signals across the heart in normal function and durring states of defibrillation.

Recent extensions: In recent years the model has been extended by adding more ion channels and a variety of receptors. This allows the model to be used for drug testing. It has also been possible to accurately account for the change in conductive properties associated with the blood vessels.

Remaining problems: The model describes an isolated heart without mechanical, hormonal or nervous contact with the rest of the body. Inputs to the heart rate variability, for instance, that is often used as an indicator of the conditions of the heart, are not included.

Everything Changes all the Time – That's what Life is

- Modeling and simulation is an efficient tool to improve our quantitative understanding of the interplay of the complicated biological processes.
- Instabilities and nonlinear dynamic phenomena (bifurcations, synchronization, chaos, etc.) are essential aspects of life.
- Instabilities are responsible for the complicated temporal variations (oscillations, spikes, bursts, etc.) that the cells and functional units use to organize their internal processes and communicate with their neighbors.
- Transitions between synchronized and desynchronized states can be part of the normal physiological regulation or represent the development of a disease.